



Calhoun: The NPS Institutional Archive

Theses and Dissertations

Thesis Collection

2013-12

Ducting conditions for electromagnetic wave
propagation in tropical disturbances from GPS
dropsonde data

Ziemba, David A.

Monterey, California: Naval Postgraduate School



Calhoun is a project of the Dudley Knox Library at NPS, furthering the precepts and goals of open government and government transparency. All information contained herein has been approved for release by the NPS Public Affairs Officer.

Dudley Knox Library / Naval Postgraduate School
411 Dyer Road / 1 University Circle
Monterey, California USA 93943

<http://www.nps.edu/library>



NAVAL POSTGRADUATE SCHOOL

MONTEREY, CALIFORNIA

THESIS

**DUCTING CONDITIONS FOR ELECTROMAGNETIC
WAVE PROPAGATION IN TROPICAL DISTURBANCES
FROM GPS DROPSONDE DATA**

by

David A. Ziemba

December 2013

Thesis Advisor:
Co-Advisor:

Qing Wang
Patrick Harr

Approved for public release; distribution is unlimited

THIS PAGE INTENTIONALLY LEFT BLANK

REPORT DOCUMENTATION PAGE			<i>Form Approved OMB No. 0704-0188</i>	
Public reporting burden for this collection of information is estimated to average 1 hour per response, including the time for reviewing instruction, searching existing data sources, gathering and maintaining the data needed, and completing and reviewing the collection of information. Send comments regarding this burden estimate or any other aspect of this collection of information, including suggestions for reducing this burden, to Washington headquarters Services, Directorate for Information Operations and Reports, 1215 Jefferson Davis Highway, Suite 1204, Arlington, VA 22202-4302, and to the Office of Management and Budget, Paperwork Reduction Project (0704-0188) Washington DC 20503.				
1. AGENCY USE ONLY (Leave blank)		2. REPORT DATE December 2013	3. REPORT TYPE AND DATES COVERED Master's Thesis	
4. TITLE AND SUBTITLE DUCTING CONDITIONS FOR ELECTROMAGNETIC WAVE PROPAGATION IN TROPICAL DISTURBANCES FROM GPS DROPSONDE DATA			5. FUNDING NUMBERS	
6. AUTHOR(S) David A. Ziemba				
7. PERFORMING ORGANIZATION NAME(S) AND ADDRESS(ES) Naval Postgraduate School Monterey, CA 93943-5000			8. PERFORMING ORGANIZATION REPORT NUMBER	
9. SPONSORING /MONITORING AGENCY NAME(S) AND ADDRESS(ES) N/A			10. SPONSORING/MONITORING AGENCY REPORT NUMBER	
11. SUPPLEMENTARY NOTES The views expressed in this thesis are those of the author and do not reflect the official policy or position of the Department of Defense or the U.S. Government. IRB Protocol number ____N/A____.				
12a. DISTRIBUTION / AVAILABILITY STATEMENT Approved for public release; distribution is unlimited			12b. DISTRIBUTION CODE A	
13. ABSTRACT (maximum 200 words) In this thesis, more than 13000 vertical profiles from GPS-enabled dropsondes, recorded from 1996 through 2010, were analyzed to determine the characteristics of electromagnetic and electro-optical ducting in the boundary layer, an environmental condition that significantly affects the propagation of radio waves. A radio wave propagation duct is formed when there are significant gradients in the humidity and temperature profiles of the atmosphere. In this study, the frequency of occurrence and the characteristics (height, depth, and strength) of a duct are identified using the temperature and humidity profiles measured by dropsondes. The identified ducts are separated based on duct types occurring in the lower troposphere: surface ducts, surface-based ducts, and elevated ducts. We further separate the duct occurrence based on the location relative to their respective storms. Based on the number of soundings in different types of tropical disturbances, we chose to further analyze duct conditions in hurricanes and tropical storms. The results suggest frequent occurrence of ducting, especially elevated ducts. This result is consistent with previous research of a similar nature. However, no preference of ducting was identified in any quadrant of the storm.				
14. SUBJECT TERMS Dropsonde, Ducting, Electromagnetic Propagation			15. NUMBER OF PAGES 77	
			16. PRICE CODE	
17. SECURITY CLASSIFICATION OF REPORT Unclassified	18. SECURITY CLASSIFICATION OF THIS PAGE Unclassified	19. SECURITY CLASSIFICATION OF ABSTRACT Unclassified	20. LIMITATION OF ABSTRACT UU	

THIS PAGE INTENTIONALLY LEFT BLANK

Approved for public release; distribution is unlimited

**DUCTING CONDITIONS FOR ELECTROMAGNETIC WAVE PROPAGATION
IN TROPICAL DISTURBANCES FROM GPS DROPSONDE DATA**

David A. Ziemba
Lieutenant, United States Navy
B.S., United States Naval Academy, 2005

Submitted in partial fulfillment of the
requirements for the degree of

**MASTER OF SCIENCE IN METEOROLOGY AND PHYSICAL
OCEANOGRAPHY**

from the

**NAVAL POSTGRADUATE SCHOOL
December 2013**

Author: David A. Ziemba

Approved by: Qing Wang, Professor
Thesis Advisor

Patrick Harr, Professor
Co-Advisor

Wendell Nuss
Chair, Department of Meteorology

THIS PAGE INTENTIONALLY LEFT BLANK

ABSTRACT

In this thesis, more than 13000 vertical profiles from GPS-enabled dropsondes, recorded from 1996 through 2010, were analyzed to determine the characteristics of electromagnetic and electro-optical ducting in the boundary layer, an environmental condition that significantly affects the propagation of radio waves. A radio wave propagation duct is formed when there are significant gradients in the humidity and temperature profiles of the atmosphere. In this study, the frequency of occurrence and the characteristics (height, depth, and strength) of a duct are identified using the temperature and humidity profiles measured by dropsondes. The identified ducts are separated based on duct types occurring in the lower troposphere: surface ducts, surface-based ducts, and elevated ducts. We further separate the duct occurrence based on the location relative to their respective storms. Based on the number of soundings in different types of tropical disturbances, we chose to further analyze duct conditions in hurricanes and tropical storms. The results suggest frequent occurrence of ducting, especially elevated ducts. This result is consistent with previous research of a similar nature. However, no preference of ducting was identified in any quadrant of the storm.

THIS PAGE INTENTIONALLY LEFT BLANK

TABLE OF CONTENTS

I.	INTRODUCTION.....	1
A.	MOTIVATION.....	1
B.	NAVAL RELEVANCE.....	2
II.	BACKGROUND.....	3
A.	NONSTANDARD EM PROPAGATION CONDITIONS.....	3
1.	Classification of Ducts.....	5
B.	THE ATMOSPHERIC BOUNDARY LAYER IN TROPICAL HURRICANE ENVIRONMENT.....	6
C.	TROPICAL CYCLONE DUCTS.....	9
III.	DATA AND METHODOLOGY.....	11
A.	THE GPS DROPSONDE.....	11
B.	THE HURRICANE DROPSONDE DATASET.....	13
C.	THE REVISED ATLANTIC HURRICANE DATABASE (HURDAT2).....	15
D.	METHODOLOGY.....	16
IV.	DATA ANALYSIS AND RESULTS.....	19
A.	IDENTIFYING EM PROPAGATION DUCTS FROM DROPSONDES.....	19
B.	DUCT LAYER CHARACTERISTICS OVERVIEW.....	23
C.	DUCTING CHARACTERISTICS IN STORM RELEVANT COORDINATES.....	26
1.	Ducting Inside Hurricanes.....	27
2.	Outside Hurricane.....	32
3.	Inside Tropical Storm.....	37
4.	Outside Tropical Storm.....	41
D.	DUCTING CONDITIONS IN DIFFERENT GEOGRAPHIC REGIONS.....	46
E.	DISCUSSIONS.....	50
V.	SUMMARY, CONCLUSIONS AND RECOMMENDATIONS.....	53
A.	SUMMARY AND CONCLUSIONS.....	53
B.	RECOMMENDATIONS.....	54
	LIST OF REFERENCES.....	55
	INITIAL DISTRIBUTION LIST.....	57

THIS PAGE INTENTIONALLY LEFT BLANK

LIST OF FIGURES

Figure 1.	Categories of refractive propagation defined from the values of $dNdz$ or $dMdz$ (from Turtton et al. 1988).	4
Figure 2.	M profiles by types of ducts. (a) surface duct, (b) surface based duct (c) elevated duct, and (d) evaporation duct. (Ding et al. 2013)	5
Figure 3.	Composite analysis result of the bulk Richardson number (Ri) with altitude and normalized radius to center of the storm. Thick black line denotes value of .25 in Ri.	8
Figure 4.	Ducting in each quadrant of the tropical cyclones separated by mean strength, mean thickness, median strength, and median thickness (from Ding et al. 2013).....	10
Figure 5.	Illustration of the components of the GPS dropsonde developed by the National Center for Atmospheric Research GPS Dropsonde (from Laing and Evans 2011)	12
Figure 6.	Locations of all quality controlled dropsondes used in this thesis. Each symbol (.) denotes the mean location of the dropsonde.....	14
Figure 7.	Tracks of all storms used in this thesis.	17
Figure 8.	An example of a dropsonde deployed in Hurricane Katrina (2005) and its relative location to the center of Katrina. The red dotted line indicates the storm track, black diamond is the location of the storm at the time of the dropsonde launch, green arcs are the radii of 64-knot winds by quadrant, blue arcs are the radii of the 34-knot winds by quadrant and the magenta dot indicates the average location of the dropsonde.	18
Figure 9.	Example of an identified surface duct. Shown here are vertical profiles of potential temperature (θ , Kelvin), specific humidity (q), modified index of refraction (M), wind speed ($wspd$, ms^{-1}), and wind direction ($wdir$). The blue line at 40 m indicates the top of the surface duct.....	20
Figure 10.	Same as in Figure 9, except for surface-based duct. The blue line at 190 meters indicates the top of the surface-based duct. There is one elevated duct at 460 m.	21
Figure 11.	A case with multiple elevated ducts: the figure depicts the vertical variation of five variables: potential temperature (Kelvin), specific humidity ($g\ kg^{-1}$), M , wind speed (ms^{-1}), and wind direction. There are two elevated ducts with tops at 600 and 5000 m, respectively.....	22
Figure 12.	Total frequency of ducting by type. The numbers on top of each bar indicate the total number of profiles with a duct of this type.	24
Figure 13.	Mean duct Height for all ducts by duct type.....	25
Figure 14.	Mean duct strength for all ducts by duct type.	25
Figure 15.	Total frequency of ducting in and out of both tropical storms and hurricanes by quadrant. The number above each column is the total soundings with ducts observed.	27

Figure 16.	Total frequency of ducting inside hurricanes by quadrant.	28
Figure 17.	Total frequency of ducting inside hurricanes for each type of duct by quadrant.	29
Figure 18.	Mean duct height and standard distribution for each type of duct inside of a hurricane by quadrant. (a) surface duct, (b) elevated high ducts, (c) surface-based duct and (d) elevated low ducts. Results in (a) are not statistically significant due to the low number of samples.	30
Figure 19.	Histogram of the distribution of duct height in the elevated low ducts (EL) inside hurricanes by quadrant. The four graphs represent the corresponding quadrants of the storm: left front (LF), left rear (LR), right front (RF), and right rear (RR).	31
Figure 20.	Same as in Figure 19, except for the elevated lower (EH) ducts inside hurricanes by quadrant.	31
Figure 21.	Same as in Figure 18, except duct strength (dM). Again, data from surface duct (a) should not be analyzed due to the small amount of data sample.	32
Figure 22.	Same as Figure 16 except for ducts outside hurricanes.	33
Figure 23.	Same as Figure 17 except for ducts outside of hurricanes.	34
Figure 24.	Figure Same as Figure 18 except for ducts outside of hurricanes.	35
Figure 25.	Same as Figure 19 except for ducts outside of hurricanes.	36
Figure 26.	Same as Figure 20 except for ducts outside of hurricanes.	36
Figure 27.	Same as Figure 21 except for ducts outside of hurricanes.	37
Figure 28.	Total frequency of ducting inside tropical storms by quadrant.	38
Figure 29.	Total frequency of ducting inside tropical storms for each type of duct by quadrant.	38
Figure 30.	Mean duct height and standard distribution for each type of duct inside of a tropical storm by quadrant. (a) surface duct, (b) elevated high ducts, (c) surface-based duct and (d) elevated low ducts. Results in (a) and (b) are not statistically significant due to the low number of samples.	39
Figure 31.	Histogram of the distribution of duct height in the elevated low (EL) ducts inside tropical storms by quadrant. The four graphs represent the corresponding quadrants of the storm: left front (LF), left rear (LR), right front (RF), and right rear (RR).	40
Figure 32.	Histogram of the distribution of duct height in the elevated high (EH) ducts inside tropical storms by quadrant. The four graphs represent the corresponding quadrants of the storm: left front (LF), left rear (LR), right front (RF), and right rear (RR).	40
Figure 33.	Mean duct height and standard distribution for each type of duct inside of a tropical storm by quadrant. (a) surface duct, (b) elevated high ducts, (c) surface-based duct and (d) elevated low ducts. Results in (a) and (b) are not statistically significant due to the low number of samples.	41
Figure 34.	Same as Figure 28 except for ducts outside of tropical storms.	42

Figure 35.	Same as Figure 29 except for ducts outside of tropical storms.	43
Figure 36.	Same as Figure 30 except for ducts outside of tropical storms.	44
Figure 37.	Same as Figure 31 except for ducts outside of tropical storms.	45
Figure 38.	Same as Figure 32 except for ducts outside of tropical storms.	45
Figure 39.	Same as Figure 33 except for ducts outside of tropical storms.	46
Figure 40.	Geographic regions of tropical disturbances as described by Neese (2010). The regions are separated by areas, which are geographically significant to the tropical storm and hurricane. Each region is dynamically different with areas, which are much less impacted by interaction with the continent and others, which are more.	47
Figure 41.	Frequency of ducting by type of duct in various geographic regions. .	49
Figure 42.	A Depiction of Ducting Climatology derived from 5 years of ECMWF Global Analysis (Engeln and Teixeira, 2004). The red box above outlines the main area of dropsondes in this study.....	51

THIS PAGE INTENTIONALLY LEFT BLANK

LIST OF TABLES

Table 1.	Dropsonde Sensor Specifications (from Hock and Franklin 1999)	12
Table 2.	Number of dropsondes examined in this thesis and the number of weather events in which dropsondes were deployed.	15
Table 3.	Overall observations of ducting in dropsondes. Number of ducts categorized in different duct types from all dropsondes. The categories are surface, surface-based, and elevated ducts. The elevated ducts are further categorized into three subsets based on the number of elevated ducts in a single profile. Note the total number of ducts exceed that of the dropsondes because of the presence of different duct types in a single profile.....	23
Table 4.	Total profiles and ducts by geographic regions.	48

THIS PAGE INTENTIONALLY LEFT BLANK

LIST OF ACRONYMS AND ABBREVIATIONS

EDH	evaporation duct height
ED	evaporation duct
EM	electromagnetic
EO	electro-optical
GPS	Global Positioning System
HURDAT2	Revised Atlantic Hurricane Database
LF	left front
LR	left rear
NHC	National Hurricane Center
RF	right front
RR	right rear
UHF	ultra-high frequency
VHF	very-high Frequency
WDIR	wind direction
WSPD	wind speed

THIS PAGE INTENTIONALLY LEFT BLANK

ACKNOWLEDGMENTS

The completion of this study was possible thanks to many people.

Professor Qinq Wang: I cannot thank you enough for your tireless patience and guidance.

Professor Patrick Harr: Thank you for your assistance and direction.

Dr. Denny Alappattu, Dr. John Kalogiros, and Ms. Mary Jordan: The incredible help and programming provided the framework for this study.

To my family, friends, and classmates: The amount of love and support received was incredible.

THIS PAGE INTENTIONALLY LEFT BLANK

I. INTRODUCTION

A. MOTIVATION

The atmospheric temperature, water vapor, and pressure have a profound influence on electromagnetic wave propagation. Consequently, there is a need to fully describe the vertical variation of these variables near-surface and in the lower troposphere. For Navy operation at the ocean surface, it is imperative to fully describe the near-surface layer in great detail in order to characterize the physical processes responsible for the formation of gradient layers that result in nonstandard propagation of electromagnetic and electro-optical waves (EM/EO) in the ultra-high frequency (UHF), very-high frequency (VHF) and microwave bands in the atmosphere. Under certain atmospheric conditions, the waves will be trapped in a vertical duct, which will increase the range that the energy normal transits.

There has been a great deal of study into the occurrence, characterization and climatology of electromagnetic ducting in the atmosphere. However, ducting conditions in and around tropical storms, hurricanes, and other major storm systems have not been characterized in sufficient detail. The only previous study on ducting in tropical cyclones and hurricanes used a relatively small dataset (Ding et al. 2013). More in-depth study with a much larger dataset is needed to fully understand the presence of nonstandard EM propagations in and near tropical disturbances, which will be the focus of this thesis research.

Currently, the physical processes in the boundary layer of hurricanes and tropical cyclones are not fully understood. The characterization of the layers will provide data into the existence of areas that enable radio transmission to propagate near the surface. There is of great interests to naval operations, for which surface duct height is of critical importance in predicting radar propagation and target detection ranges.

The marine atmospheric boundary layer is extremely important to Navy operations as surface based operations take place in the boundary layer. There is limited data analysis of ducting in multiple environments. An understanding of the boundary layer in the tropical environment will contribute to further knowledge of and the conditions which influence ducting and hence will increase the current knowledge base on the behavior of EM/EO propagation through the lower atmosphere.

B. NAVAL RELEVANCE

In order to assess and fully exploit the areas in which our navy operates there must be a full understanding of the environment. The knowledge of the depth and locations of ducts, especially surface ducts, are a necessity to assess the true ranges of both our and the adversaries radar and communications propagation ranges for both offensive and defensive operations. The occurrence or absence of a duct will greatly modify the range of different operational systems such as radio communications, radar navigation, weapon, and various sensors, each of which vary in the heights of the antenna and target and respond differently to varying duct heights.

Although very few operational assets will be in the areas of an active tropical disturbance, some do operate in the outskirts of a hurricane or a tropical storm. Submarines may operate both in and around tropical disturbances. During hurricane avoidance procedures fleet assets will be in the area of the data sets being used. During these tropical storms and hurricanes submarines may continue to operate in the area of storm force winds. It is important to know the influences of ducts due to the surface based location of the submarine sensors. Ships avoiding hurricanes will also have sensors located within the boundary layer and will be impacted by the surface ducts. Elevated ducts are more influential on aviation operations when aircraft are located in the trapping layer aloft.

II. BACKGROUND

A. NONSTANDARD EM PROPAGATION CONDITIONS

The propagation of electromagnetic and electro-optical waves (EM/EO) along a certain path in the atmosphere is dependent upon the vertical variation of atmospheric conditions above the sea-surface. The key atmospheric property that determines radio wave propagation is the index of refraction, n , defined as $n = \frac{c}{v}$, where c is the speed of light in a vacuum (free space), and v is the speed of light in a homogeneous medium (Battan 1973). For convenient, the index of refraction is usually replaced by a “radio refractivity,” N , defined as $N = (n - 1) \times 10^6$. In this thesis, the term index of refraction will be the radio refractivity by default.

The radio refractivity N is associated with the atmospheric parameters in the following expression (Bean and Dutton, 1968):

$$N = 77.6 \frac{P}{T} - 5.6 \frac{e}{T} + 3.75 \times 10^5 \frac{e}{T^2} \quad (1)$$

where p is air pressure in millibars, T is temperature in Kelvin, e is the vapor pressure in millibars. The index of refraction calculated in Equation (1) is used to characterize radio propagation with respect to the radius of the Earth. Practically, the modified refractive index, M , is defined to include the effects of the curvature of the Earth:

$$M = N + \frac{z}{R \times 10^{-6}} = N + 0.157z \quad (2)$$

where z is height in meters above the surface, and R is the radius of the Earth (6.37×10^6 meters) (Battan, 1973). It is clear from Equation (1) that the refractive property of the atmosphere is affected by temperature, water vapor, and atmospheric pressure.

In general, there are four categories of refractive propagations depicted in Figure 1 (Turton et al. 1988): sub-refraction, standard refraction, super-refraction, and ducting. These refractive conditions are defined by the vertical gradient of index of refraction N or M as illustrated in Figure 1. Of major concern to this

thesis are the ducting conditions when the curvature of the ray becomes greater than that of the earth so that the ray will be bent to such an extent that it intersects the surface, a process that is generally referred to as “trapping” (Turton et al. 1988). The trapping layer is thus defined in which the ray is bent back downward, which happens when $dN/dz < -157$ or $dM/dz < 0$. Significant humidity decrease and temperature increase with height (or vertical gradient of humidity and temperature) create trapping layers and the formation of a duct. These anomalous conditions allow propagation to longer distances compared to those in a standard atmosphere.

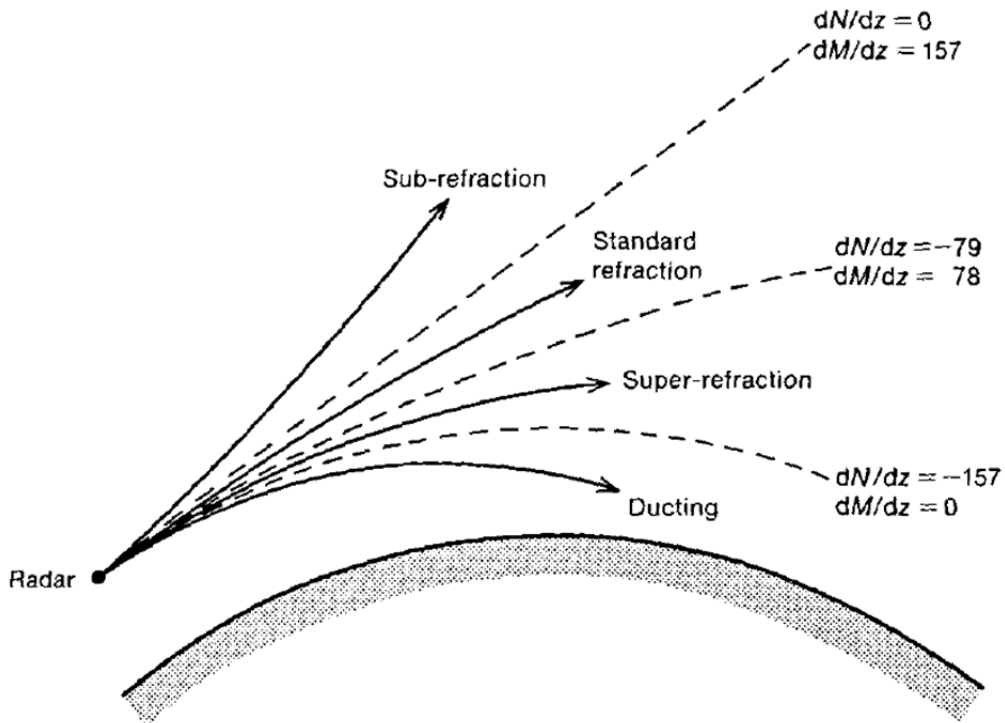


Figure 1. Categories of refractive propagation defined from the values of dN/dz or dM/dz (from Turtton et al. 1988).

1. Classification of Ducts

When trapping occurs, the EM wave is confined by a layer called the duct whose top is at the top of the trapping layer. The duct associated with the trapping layer extends below the trapping layer base to the level where M is higher than the minimum value at the top of the trapping layer. Figure 2 shows the four types of ducts: surface, surface-based, elevated and evaporation duct. The surface duct (Figure 2a) is defined as those ducts whose trapping layer base is at the surface. In this case, the depth of the trapping layer is the same as that of the duct.

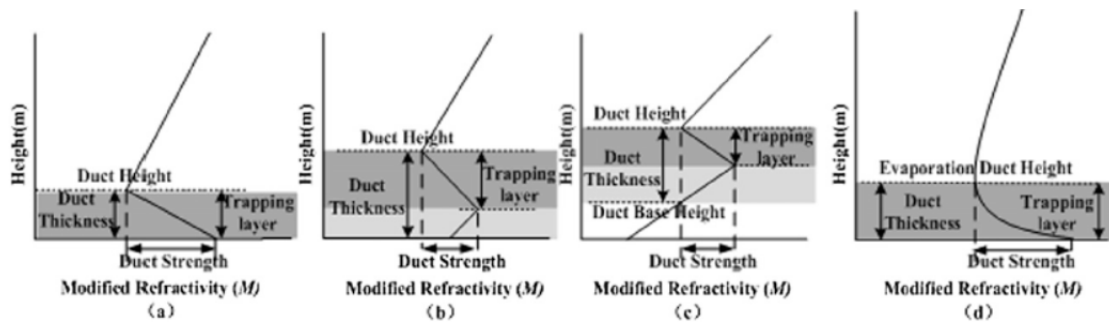


Figure 2. M profiles by types of ducts. (a) surface duct, (b) surface based duct (c) elevated duct, and (d) evaporation duct. (Ding et al. 2013)

The surface duct (Figure 2a) often occurs due to a warm and dry air mass flowing over a cooler body of water. The warm air over cold water forms a surface-based inversion with moisture decreasing rapidly with height, resulting in substantial negative M gradient in the lowest levels (Battan, 1973). Surface ducts are also caused by subsidence in storms. The air descends and has high humidity due to the precipitation evaporation within the cell. The evaporation duct (Figure 2d) is a subset of a surface duct. Evaporation ducts are based at the surface where there is a strong gradient of both humidity and temperature due to evaporation at the air-sea interface. They are often found over warm water where substantial surface evaporation creates a humidity gradient just above the sea surface (Babin, 1996). Typically, the depth of an evaporation duct is between a

few and tens of meters in depth, but may dramatically increase depending on the air mass, the temperature of the water, and the structure of the atmospheric boundary layer.

The elevated ducts (Figure 2c), do not extend to the surface. Elevated ducts often occur due to subsidence of air masses, with elevated inversions of moisture and temperature aloft especially near areas of upwelling along the coasts (Engeln and Teixeira 2003). Elevated ducts can also form due to strong daytime surface heating where strong turbulence eddies are capped by an inversion aloft. This type of ducting has been observed up to 4 km but is usually below 2 km. The surface based duct (Figure 2b) occurs when an elevated duct has a strong trapping layer which creates a duct thick enough to extend to the surface.

B. THE ATMOSPHERIC BOUNDARY LAYER IN TROPICAL HURRICANE ENVIRONMENT

Ducting often occurs in areas where there is a temperature inversion concurrent with sharp moisture decrease through the layer. Such vertical stratification in temperature and moisture often occurs at the top of the boundary layer. Defining the boundary layer height is not a trivial task and invokes much debate especially in the highly disturbed tropical environment. Since the boundary layer plays an integral part in the overall thermodynamic processes of a tropical disturbance, clearly defining its boundary layer is crucial to a full understanding of the development of the system. Smith and Montgomery have made extensive studies on a dynamical definition of the boundary layer based on the distribution of the agradient flow (Smith and Montgomery 2010). Diagnostic models and numerous studies have been produced to define the heights and intensity of the tropical cyclone boundary layer using slab and height models by Kepert (2010). Zhang et al. (2011) used an observational study to describe the height scales of the hurricane boundary layer that used data from 794 GPS dropsondes from 1997 to 2005. Because of the importance of boundary layer structure in momentum and moisture exchange in hurricane environment, correct

representation of the boundary layer processes in numerical models to properly forecast changes in hurricane movement and intensity is of vital importance. However, definition and identification of the boundary layer height remains controversial. Zhang et al. (2011) made an effort to characterize the hurricane boundary layers using observational data in 13 named hurricanes.

The boundary layer is defined by the characteristics of the lower troposphere which is directly influenced by the surface and a time scale of less than or equal to an hour (Zhang et al. 2011). Using the given definition they attempted to use the height where measured turbulent fluxes became negligible as the boundary layer height. It follows that the height of the boundary layer can be characterized by the bulk Richardson number (Ri_b), as in the case with many in numerical models.

$$Ri_b = \frac{\left(\frac{g}{\theta_{vs}}\right)(\theta_{vs} - \theta_{vH})(H - z_s)}{(U_H - U_s)^2} \quad (3)$$

Where Ri_b is the Richardson number between an atmospheric level z_s and the boundary top H . H is the boundary layer top, θ_{vH} and θ_{vs} are the virtual potential temperature at H and z_s , and $U_H - U_s$ is the change in the wind speed (Zhang et al. 2011). Since all variables in the bulk Richardson number are measured by or derived from dropsonde data, dropsonde measurements can be used to calculate the bulk Richardson number at all levels of measurement.

The Zhang et al. (2011) study used three height scales to determine the boundary layer depth. Their data analysis showed the height of the low level wind jet distinctly with a logarithmic decrease in wind speed with decreasing height. The inflow of these storms was greatest at 150 meters above sea level (note they found in this study that inflow layer depth is above the height of the maximum tangential winds.) The analysis confirmed with previous studies that the boundary layer heights decreased closer to the center of the storm. The mixed layer is shallower in the squall lines and rain bands due to the convective downdrafts transporting cool dry air to the low-levels of the boundary layer (Zhang et al. 2011). They found that the bulk Richardson (Figure 3) may not be the best

parameter to describe the actual height of the boundary level as compared to the boundary layer height determined from the turbulent fluxes and the vertical transports.

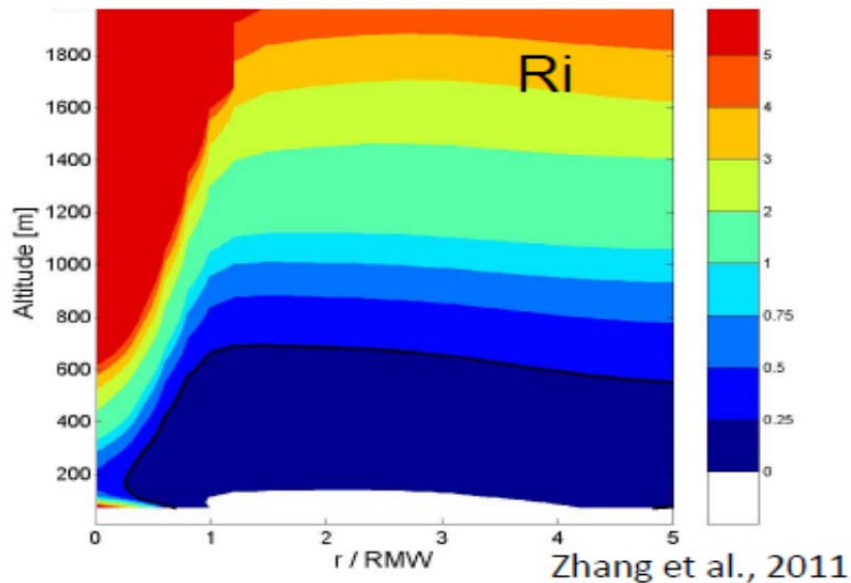


Figure 3. Composite analysis result of the bulk Richardson number (Ri) with altitude and normalized radius to center of the storm. Thick black line denotes value of .25 in Ri.

The dynamical height scale of the hurricane boundary layer is defined using the inflow layer depth. Inflow in the boundary layer is due to the imbalance of pressure gradient force, Coriolis and centrifugal force. The inflow layer depth is at the height where the radial velocity is 10% of the peak inflow (Zhang et al. 2011). The variations in depth between using a Ri criterion of 0.25 and the depth using inflow layers indicates that there is not just one depth that describes the boundary layer. Inflow layers changed dramatically with respect to the category of the hurricane being studied. In stronger hurricanes (i.e., category 4–5) the inflow layer depth was much higher than in lower categorical storms. Inflow increases with decreasing radius in stronger storms. It was theorized this occurs due to stronger storms having warmer cores (Zhang et al. 2011).

C. TROPICAL CYCLONE DUCTS

There have not been many studies focused on the occurrence of EM wave ducts in gale wind conditions with the exception of Ding et al. (2013). Using GPS dropsonde data, Ding et al. (2013), conducted an analysis of dropsonde vertical profiles in tropical cyclones to evaluate the EM propagation conditions in such environment. Their study used a total of 357 dropsondes over a period from September 2003 to September 2004, deployed in tropical cyclones located southeast of China and Taiwan. Based on the resultant M profiles, the authors characterized various properties of EM ducts, including duct type, duct height, duct thickness, and the strength of the duct.

The observational study by Ding et al. (2013) found that of 357 dropsondes there were 212 cases of ducting conditions, an occurrence of 59%. Of the 212 dropsondes which displayed ducting, about half of the profiles exhibited multiple layers of ducting. Their findings indicated that the ducts on the left side of the hurricane track exhibited stronger and thicker ducts than those on the right side of the tropical cyclone. Ding et al. (2013) stated that the rush of cool dry air on the north and left of the cyclone and the ensuing subsidence associated with the locations are the cause of the increase in ducting thickness and strength.

Surface ducts did not often occur in the observational study. Ding et al. found only 5% of profiles exhibited a surface duct. The data displayed overall duct strength and thickness was weak and not deep for both elevated and surface ducts. They summarized that the reason was consistent with the theory that the tropical cyclone environment was hostile to the formation of ducts.

Ding et al. (2013) further separated the identified ducts into three categories of ducts by strength: strong ducts ($dM > 10M$), moderate ducts ($5M < dM \leq 10M$) and weak ducts ($dM \leq 5M$). The weak ducts proved to be dominant inside tropical cyclones. Strong ducts occurred more outside the tropical system. They surmised that these findings were consistent with the theory that the

conditions inside a cyclone did not enable formation of ducts. The large number ducts outside the system was due to interaction with other synoptic events which effectively enhanced the ducts in outside locations (Ding et al. 2008).

Ding et al. (2013) further evaluated ducting occurrence by location of the profiles with respect to the track of the storm. The authors separated the data by the left-front (LF), left-back (LB), right-front (RF), and right-back (RB) side of the track of the system to determine if there were differences in the distribution of ducts by quadrant. Their study found that the majority of the ducts occurred on the left side of the track, although there was not an in depth discussion on the statistical significance of the findings.

Figure 4 shows the results from Ding et al. (2013) on ducting strength and duct layer thickness in each quadrant of the tropical cyclone (Figure 4). The findings displayed the strength and thickness of ducting is greatest on the left side of tropical cyclones. The intensities were broken down by six grades of tropical depression, tropical storm, severe tropical storm, typhoon, severe typhoon, and super typhoon. The 212 incidents of ducting were separated by 41% in a typhoon, 30% in a severe typhoon, 11% in a tropical storm, 10% in a super typhoon, and 8% in severe typhoon.

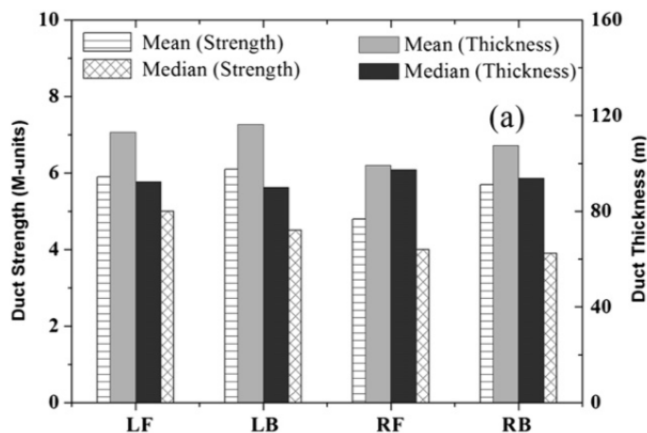


Figure 4. Ducting in each quadrant of the tropical cyclones separated by mean strength, mean thickness, median strength, and median thickness (from Ding et al. 2013)

III. DATA AND METHODOLOGY

A. THE GPS DROPSONDE

The measurement device used in this study to sample the atmospheric environment is the GPS dropsonde originally developed at the National Center for Atmospheric Research (Hock and Franklin 1999). The dropsonde provides a high resolution description of atmospheric conditions of the environment it passes through. The addition of GPS dramatically improved the resolution of winds in the data. Since its inception, dropsondes have been widely used especially in hurricane environment for the purpose of improving forecasts of hurricane track and intensity. The forecast error was shown to be reduced and the improvement in the dropsonde system would improve accuracy of forecasts (Hock and Franklin 1999).

Hock and Franklin (1999) gives a detailed description of the dropsonde and its data acquisition system. A dropsonde is a cylindrical device with multiple sensors which is deployed from aircraft at altitudes. Figure 6 gives a detailed view of the GPS dropsonde. The dropsonde (Figure 5) uses multiple sensors to resolve the profiles of temperature and humidity of the atmosphere, while GPS data provide the position information from which wind speed and velocity were derived. The use of GPS represents the major advance in resolution and accuracy over the previous generation of dropsondes, which did not use GPS. The new era of GPS enabled dropsondes increased the resolution of the dropsonde data by an order of magnitude from 150 meters down to 5 meters. The precision of the GPS winds are approximately .2 m/s (Hock and Franklin 1999).

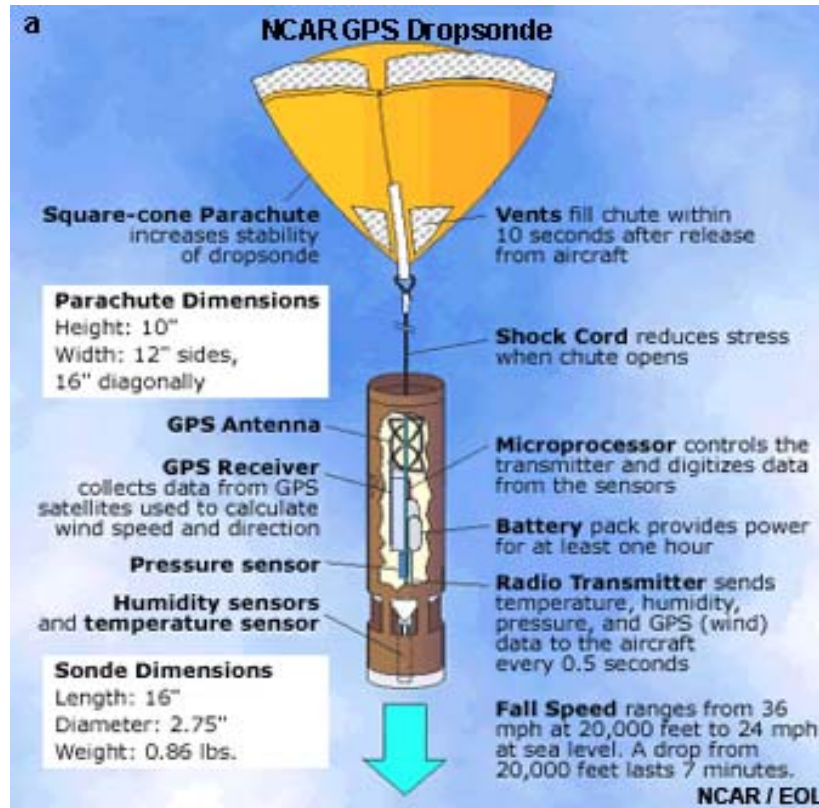


Figure 5. Illustration of the components of the GPS dropsonde developed by the National Center for Atmospheric Research GPS Dropsonde (from Laing and Evans 2011)

When a dropsonde exits an aircraft a parachute is deployed to stabilize and slow the dropsonde for its motion through the atmosphere. The dropsonde data is sent back to the receivers on the aircraft in real time. Table 1 gives the sampling accuracy and resolution of the key parameters from a dropsonde.

	Range	Accuracy	Resolution
Pressure	1080–100 hPa	± 1.0 hPa	0.1 hPa
Temperature	-90 to +60 C	± 0.2 C	0.1 C
Humidity	0–100%	± 5%	1.0%
Horiz Wind	0–200 m/s	± 0.5 m/s	0.1 m/s

Table 1. Dropsonde Sensor Specifications (from Hock and Franklin 1999)

Dropsonde data go through several levels of processing and data quality control through the inflight data processing software and post processing. The quality control procedures were implemented to ensure the accuracy of each sounding profiles for future data analyses or for use in model evaluation and assimilation. The goal of the onboard data processing system is to use automated algorithms to identify apparently erroneous data. The post-flight corrections and quality control are also applied to each dropsonde profile with corrections for wind shear and thermal sensor lags. Any unresolvable scales of heights and geopotential height routines are integrated to filter out and eliminate aliasing (Hock and Franklin 1999).

B. THE HURRICANE DROPSONDE DATASET

From 1996 through 2012 the United States Air Force and the National Oceanographic and Atmospheric Administration (NOAA) flew numerous missions with multiple aircraft into and around tropical cyclones, hurricanes, and other categories of tropical and mid-latitude disturbances. During these years over 20,000 individual dropsondes were released from aircraft, belonging to both the military and civilian entities. There has been a recent effort on quality control (QC) of the sounding data conducted at the National Center for Atmospheric Research (NCAR). The QC'd data set is made available to the science community to fit for various research need related to tropical disturbances using the valuable resource of the past many years.

This thesis study utilized the quality controlled hurricane dropsonde dataset to study the characteristics of EM propagation conditions in and around tropical disturbances such as hurricanes and tropical storms. Figure 6 depicts the location of all available dropsonde with correct latitude and longitude information. The majority of the soundings were made in the Gulf of Mexico and the western Atlantic Ocean. The soundings display the use of dropsondes to fully describe storms which may impact the United States. The majority of the soundings were

made by three main aircraft: the NOAA WP-3D, a NOAA G-IV Gulfstream Jet, and the USAF WC-130J.

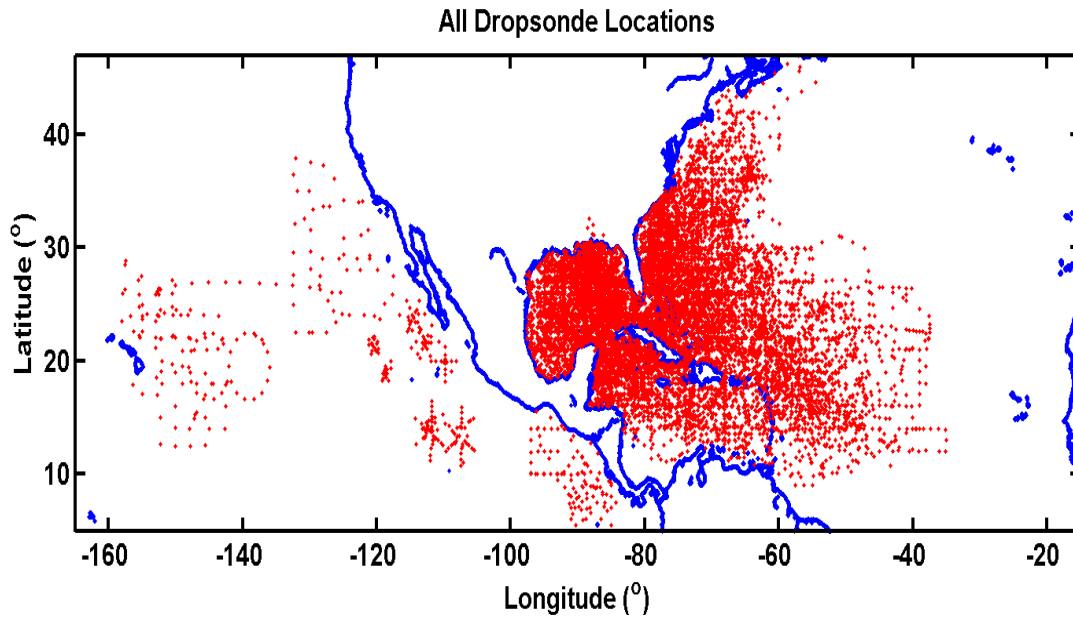


Figure 6. Locations of all quality controlled dropsondes used in this thesis. Each symbol (.) denotes the mean location of the dropsonde.

Further investigation into the dataset reveals more details of the dropsonde time and locations and especially the tropical disturbances associated with each of the dropsonde. Table 2 gives an overview of the number of soundings from each year between 1996 and 2012 and number of weather events in which the dropsondes were deployed. In the period of 17 years, a total of 13664 profiles were obtained from dropsonde deployments in 120 of various tropical disturbances.

Years	Number of Events	Number of Dropsondes
1996	7	68
1997	7	388
1998	7	1124
1999	11	1105
2000	8	311
2001	7	709
2002	7	948
2003	5	769
2004	5	1332
2005	13	2291
2006	5	470
2007	6	361
2008	8	1302
2009	5	540
2010	9	952
2011	7	278
2012	3	716
Total	120	13664

Table 2. Number of dropsondes examined in this thesis and the number of weather events in which dropsondes were deployed.

C. THE REVISED ATLANTIC HURRICANE DATABASE (HURDAT2)

In order to examine the variability of the ducting conditions relative to the storm it sampled, we obtain storm track data from the revised Atlantic Hurricane Database (HURDAT2) produced by the National Hurricane Center. The data is compiled using all observations which include real-time data and post-analysis. There have been several iterations of HURDAT formatting, but current formats contain a six hour update of storm track with cyclone number, name, date-time group, status of system (tropical depression, tropical storm, hurricane, extratropical cyclone, subtropical depression, subtropical storm, a low of no category, tropical wave, disturbance or not named), location of center of storm, max sustained wind, minimum pressure. Starting in 2004, the hurricane data also included the radii of 34, 50, and 64 knot winds given by quadrant. The data can now be used to determine the extent of the category force winds for both tropical

storms (34 knot radius) and hurricanes (64 knot radius). The ability to reanalyze the storms by quadrant is of great importance for this thesis.

D. METHODOLOGY

MATLAB was used to analyze the dropsonde dataset. The original QC'd dropsonde data were in ASCII format organized in several layers of subdirectory by year, storm, type of data, and the airplane from which the dropsonde was deployed. A MATLAB code was developed to read all profiles and store the profiles by year in a MATLAB structure array with all relevant information written in the fields of the structure array. In do this, relevant variables such as the modified refractive index was also calculated and stored as one of the field of the profile structure array.

A separate MATLAB code was developed, thanks to Dr. John Kalogiros of National Observatory of Athens (NOA), to automatically detect the ducting layer characteristics for each dropsonde profiles based on the vertical gradient of M profile. The duct detection code also determines the types of ducts (surface, surface based and elevated ducts) and output duct strength, thickness, duct layer top and base, and the trapping layer base. The criterion for minimum duct strength is 2 M unit by reasoning that a layer with an M difference less than 2 M unit would not likely have much impact on ducting.

Once a duct was identified in a profile, there was a need to group the duct by type. Three types of ducts can be identified from this dataset in this thesis: surface duct, surface-based duct, and elevated duct. The surface ducts may include the evaporation duct as the fourth duct type in Figure 2; however, we were unable to differentiate the two types from the given data.

The HURDAT2 dataset was read in conjunction with the dropsonde data so that storm relative coordinates of each dropsonde were obtained to include the radius to the storm center and azimuth angle relative to the direction of storm motion. Figure 7 shows the complete track of each storm with dropsonde deployment.

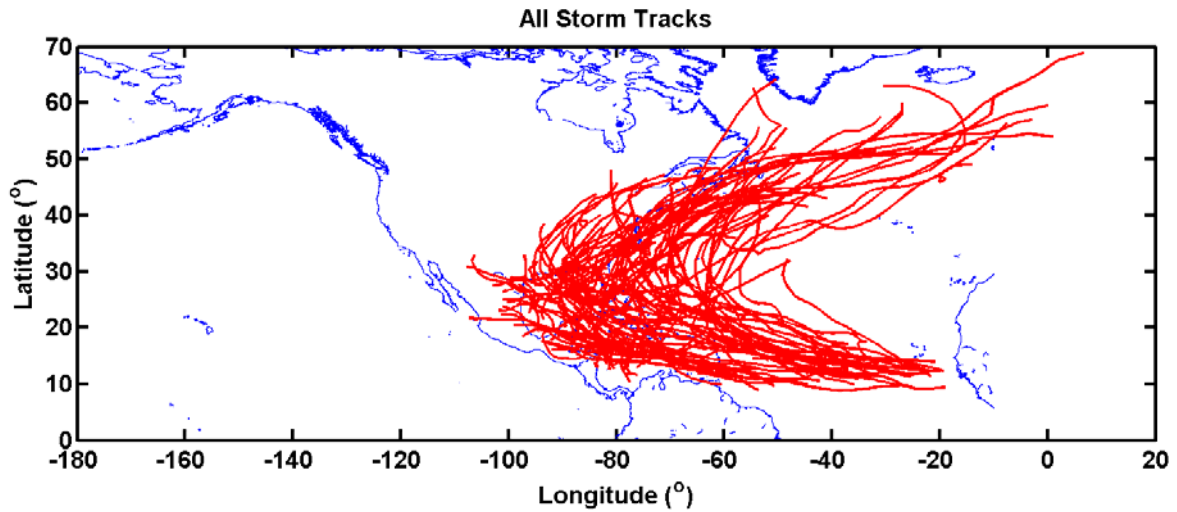


Figure 7. Tracks of all storms used in this thesis.

It is seen that the majority of the storm are in the Gulf of Mexico and along the western Atlantic Ocean. There were a few sampled storms in the Eastern Pacific ocean.

The relative location of the dropsonde to the storm enabled a comparison to the environment it was deployed. Figure 8 shows an example of a single dropsonde, its associated storm track (Hurricane Katrina, 2005), and the center of the storm at the time of dropsonde deployment. The radius of 34 kt and 64 kt wind for each quarter is also illustrated in this figure. This type of association was conducted for every dropsonde which was associated with a tropical storm or hurricane.

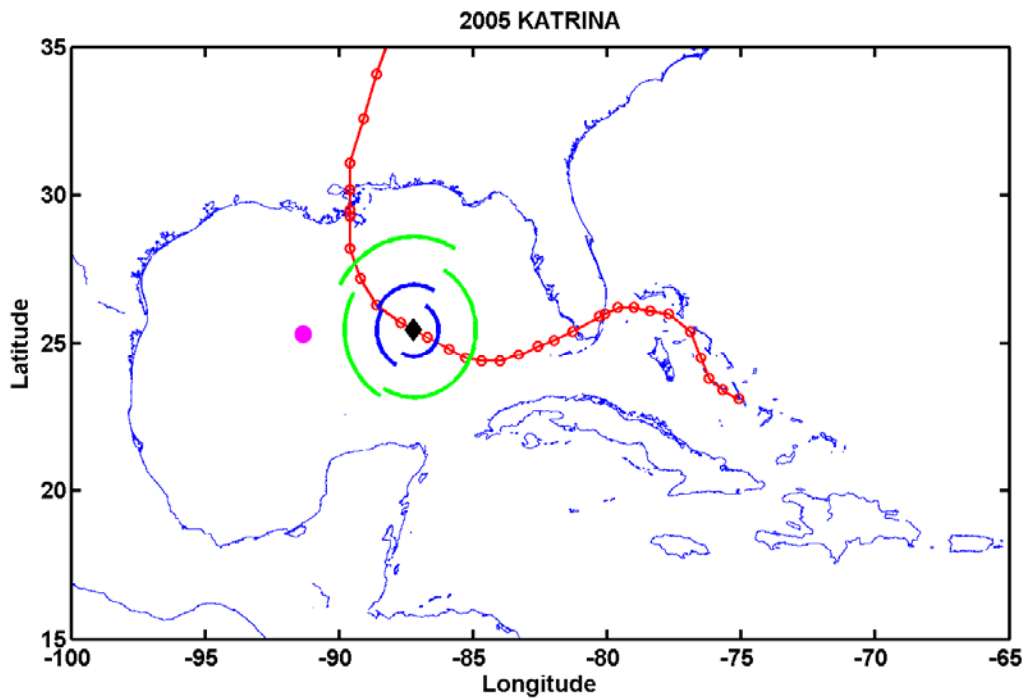


Figure 8. An example of a dropsonde deployed in Hurricane Katrina (2005) and its relative location to the center of Katrina. The red dotted line indicates the storm track, black diamond is the location of the storm at the time of the dropsonde launch, green arcs are the radii of 64-knot winds by quadrant, blue arcs are the radii of the 34-knot winds by quadrant and the magenta dot indicates the average location of the dropsonde.

IV. DATA ANALYSIS AND RESULTS

A. IDENTIFYING EM PROPAGATION DUCTS FROM DROPSONDES

The goal of this study is to characterize ducting conditions in tropical disturbances. The data from both the HURDAT2 and dropsonde measurements must be parsed and examined for this purpose. The first step in data analysis of this project was to identify ducts from the M profiles calculated from the dropsonde measurements of pressure, temperature, and relative humidity

MATLAB was used as major tool for analyzing the dropsonde dataset. The original QC'd dropsonde data were in ASCII format organized in several layers of subdirectory by year, storm, type of data, and the airplane from which the dropsonde was deployed. A MATLAB code was developed to read all profiles and store the profiles by year in a MATLAB structure array with all relevant information written in the fields of the structure array. In do this, relevant variables such as the modified refractive index was also calculated and stored as one of the field of the profile structure array.

A separate MATLAB code was developed, thanks to Dr. John Kalogiros of National Observatory of Athens (NOA), to automatically detect the ducting layer characteristics for each dropsonde profiles based on the vertical gradient of M profile. The duct detection code also determines the types of ducts (surface, surface-based and elevated ducts) and output duct strength, thickness, duct layer top and base, and the trapping layer base. The criterion for minimum duct strength is 2 M unit by reasoning that a layer with an M difference less than 2 M unit would not likely have much impact on ducting.

The duct detection code automatically denotes the duct type for each identified duct in every profile, including surface duct, surface-based duct, and elevated duct. The surface ducts may include the evaporation ducts, as there is no direct way of separating the two types automatically.

An example of a sounding with a surface duct is shown below in Figure 9. This sounding shows a surface duct up to 40 meters where there is a moist layer near the sea-surface. The profile displays a well-mixed boundary layer up to 600 meters, which after the boundary layer height does not have a duct. The profile for the surface duct is associated with shear, wind speeds from 26 ms^{-1} to 36 m/s , and little variability of wind direction through the lowest 1000 meters of the sounding.

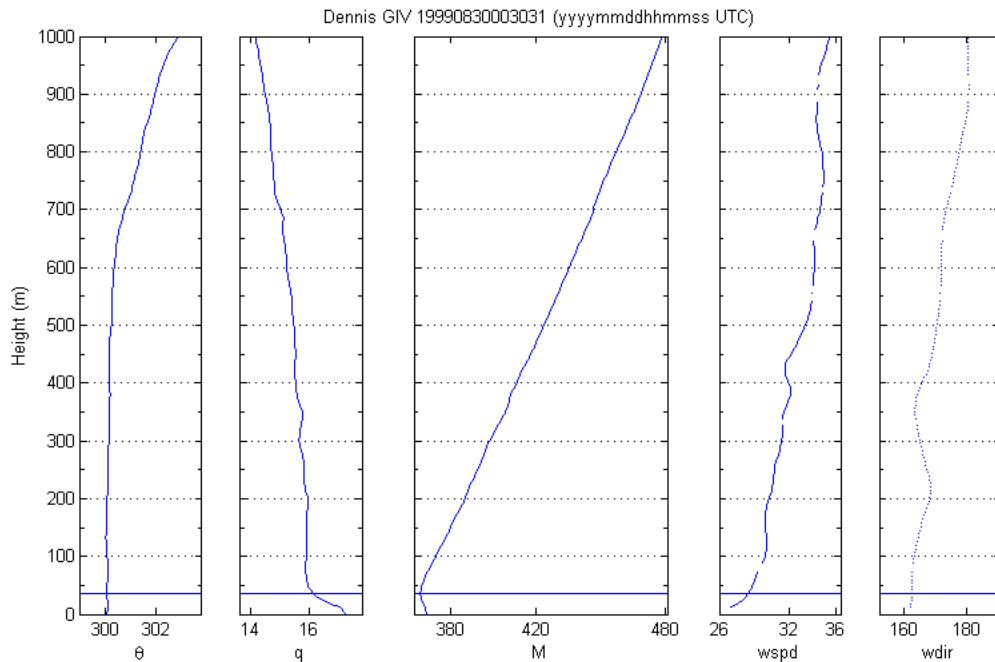


Figure 9. Example of an identified surface duct. Shown here are vertical profiles of potential temperature (θ , Kelvin), specific humidity (q), modified index of refraction (M), wind speed ($wspd$, ms^{-1}), and wind direction ($wdir$). The blue line at 40 m indicates the top of the surface duct

The surface-based duct (Figure 2b) was the second group of ducts identified in this study. The surface-based duct as defined earlier has an M profile that is elevated above the surface of the ocean, but the minimum M value at the top of the trapping layer is the lowest in the layer below. Figure 10 displays an example of the surface-based duct. The M profile starting at the surface is nearly identical to the example given in Figure 2b earlier. The M profile begins with a positive gradient near the surface and negative gradient starting at

50 meters above the surface. The top of the duct is concurrent with the change in the humidity and appears to correspond to the top of the boundary layer. The top of the duct is located slightly below the strongest wind speed in the sounding.

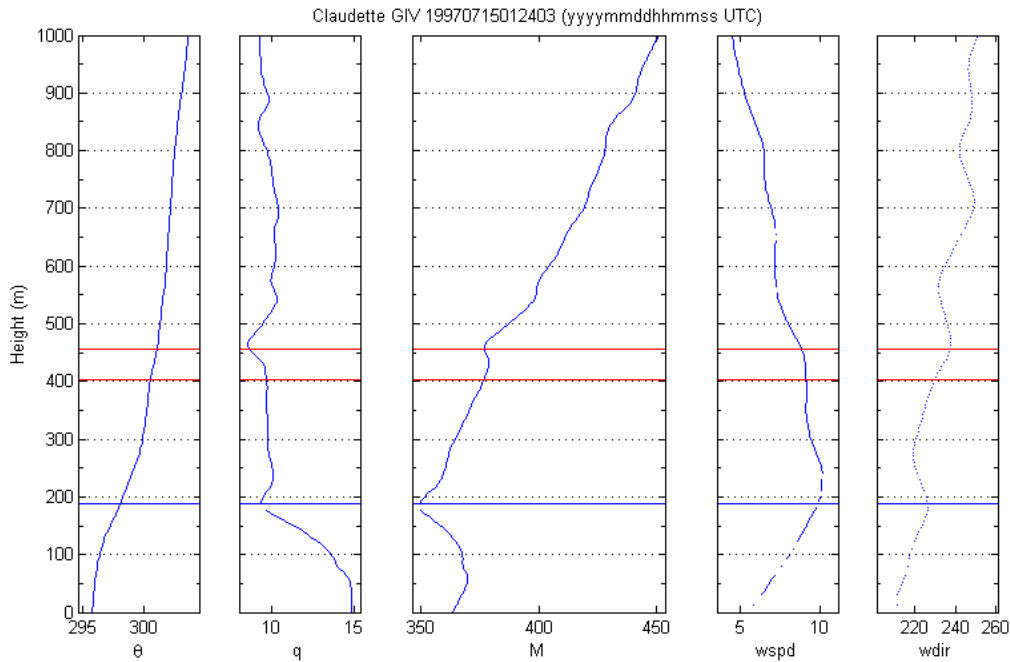


Figure 10. Same as in Figure 9, except for surface-based duct. The blue line at 190 meters indicates the top of the surface-based duct. There is one elevated duct at 460 m.

After investigating numerous profiles elevated ducts often occurred more than once. The elevated ducts were above surface-based ducts, surface ducts and with other elevated ducts. The dataset displayed a tendency of numerous elevated ducts occurring at lower altitudes then followed by a second at higher altitudes. The observed multiple ducting events in a single sounding often resembled Figure 11. The sounding has a single elevated duct at 600 meters with another elevated duct at 5000 meters. The profile of Figure 11 has a well-mixed boundary layer up to the base of the duct. There was nearly constant humidity, wind speed and wind direction below the base of the duct. The boundary layer height seems to be at the base of the trapping layer since there is a dramatic change in the humidity. The second elevated duct with a duct height

of 5000 meters occurs at location where humidity again rapidly decreases to nearly 0, and there is a dramatic increase in wind speed at the top of the duct. Apparently, the 5000 meter duct is displaying the top layer with hurricane influence.

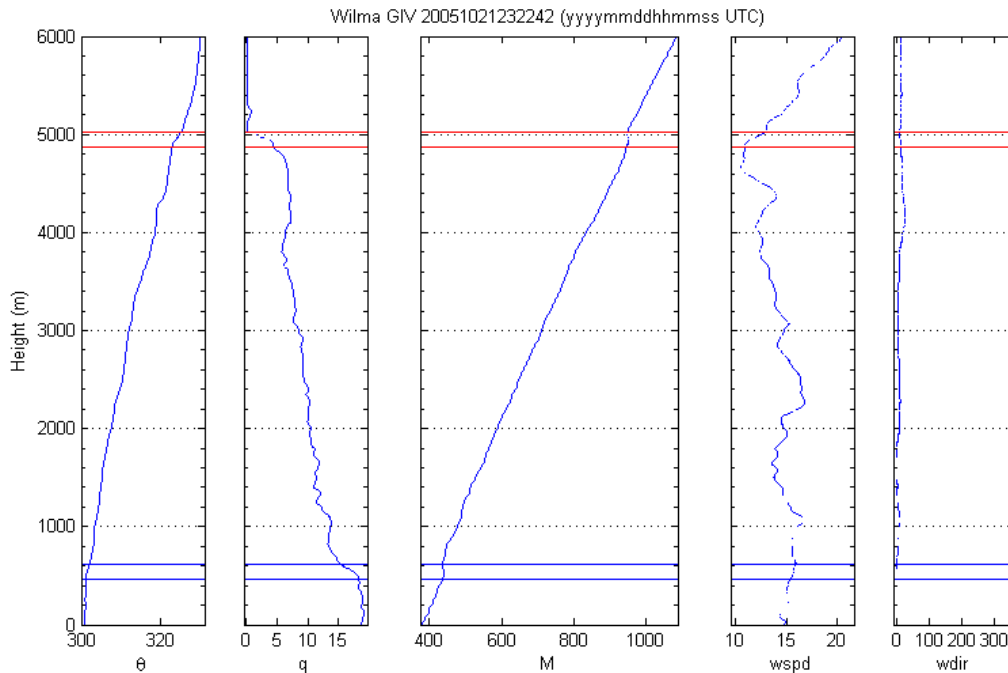


Figure 11. A case with multiple elevated ducts: the figure depicts the vertical variation of five variables: potential temperature (Kelvin), specific humidity (g kg^{-1}), M, wind speed (ms^{-1}), and wind direction. There are two elevated ducts with tops at 600 and 5000 m, respectively.

The multiple elevated ducts were consistently observed. However, we will not discuss the occurrence of every duct layers except for the lowest and the highest, referred to as elevated low and elevated high ducts, respectively. For those profiles with a single duct with elevation higher than 2000 m, we group them into the elevated high duct category. Similarly, those profiles with a single and low elevated layer, lower than 2000 m, they are grouped into the elevated low category. It is general known that ducts with altitudes greater than 2.5 km may not affect practical RF propagation. However, we intend to keep the

elevated high duct category since it appears to indicate well the vertical extent of the hurricane-affected layer.

B. DUCT LAYER CHARACTERISTICS OVERVIEW

The initial analysis of the dropsonde data was to identify all ducts occurring in the entire dataset and the number of ducts in each duct type (Figure 2). The results are summarized in Table 3. The surface duct was found to have 300 total occurrences, which indicate a frequency of 2% of all 13600 soundings with a surface duct. Surface-based ducts existed in 4.8% of all ducts. The overall frequency of ducting was 60.7% from all dropsondes. As seen in the previous section, multiple ducts can occur in the same profile due to moisture variability, the most ducts observed in a single sounding was nine elevated ducts. It was also found that the majority of surface and surface-based ducts had an elevated duct in the same sounding.

	Number of Ducts	Totals
Surface Ducts Only	117	
Surface Ducts with Elevated Ducts	183	
Total Surface Ducts		300
Surface-Based Ducts Only	312	
Surface-Based Ducts With Elevated Ducts	356	
Total Surface-Based		668
Single Elevated Ducts	3577	
Two Elevated Ducts In A Sounding	2228	
More Than Two Elevated Ducts In A Sounding	2061	
Total Elevated Ducts		15866
Total Ducts		16834

Table 3. Overall observations of ducting in dropsondes. Number of ducts categorized in different duct types from all dropsondes. The categories are surface, surface-based, and elevated ducts. The elevated ducts are further categorized into three subsets based on the number of elevated ducts in a single profile. Note the total number of ducts exceed that of the dropsondes because of the presence of different duct types in a single profile.

Figure 12 displays the total frequency of ducting by type of duct. The results show the majority of ducting occurs in elevated lower and elevated high ducts. The frequency will be further investigated for other criteria.

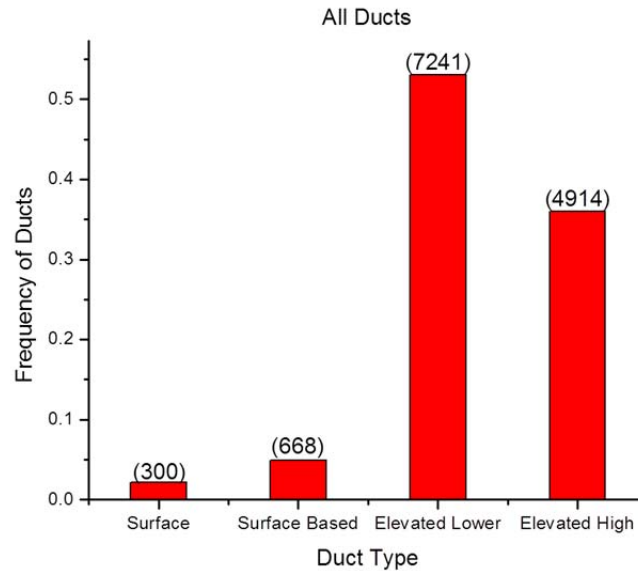


Figure 12. Total frequency of ducting by type. The numbers on top of each bar indicate the total number of profiles with a duct of this type.

The duct height (Z_d) and duct strength (dM) are two important duct attributes to be discussed in detail next. Using the M profile determining the height of the duct will describe both the structure of the tropical environment as well as the altitude of the duct for tactical significance. The mean duct height is shown in Figure 13.

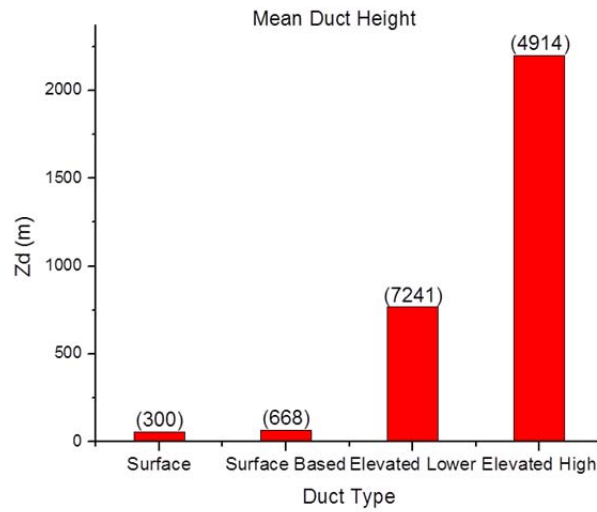


Figure 13. Mean duct Height for all ducts by duct type.

The mean duct strength displayed in Figure 14, for all types of ducts, is similar to those in Ding et al. (2013). The duct strength of approximately 6 M-units for both the surface-based and elevated lower ducts is consistent with the expected values of surface and elevated ducts in the atmosphere as seen in the climatology study by Engeln and Teixeira (2004).

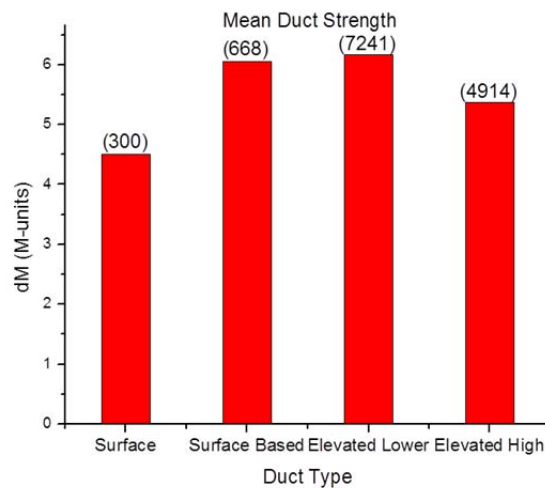


Figure 14. Mean duct strength for all ducts by duct type.

C. DUCTING CHARACTERISTICS IN STORM RELEVANT COORDINATES

The following section is an analysis of the ducting for the tropical storms and hurricanes that involved dropsonde soundings in this dataset. The asymmetric variability of the tropical environment has been discussed in Ding et al. (2013), which shows a higher likelihood of ducting on the left side of tropical storms and hurricanes. It is generally believed that the left side of tropical storms and hurricane is the most conducive to the duct environment because of the left side of the storm is more likely to interact with the land surface and is conducive to dry air intrusion into the storm. The statistics in Ding et al. (2013), showing greater frequency of ducting on the left of the tropical cyclones, seemed to be consistent with the common notion. Ding et al. (2013) further described that the left side had higher ducting heights and greater duct strength (dM) in all types of storms and ducting by category.

Figure 15 shows overall frequency of ducting for soundings in and out of tropical storms and hurricanes in the dropsonde dataset. It is apparent that the left side of the systems is not the most conducive area for ducting to occur. The data for the tropical storms and hurricanes was investigated by quadrant of the system relative to the best track data from HURDAT2. The quadrants are named: left front (LF), left rear (LR), right front (RF), and right rear (RR).

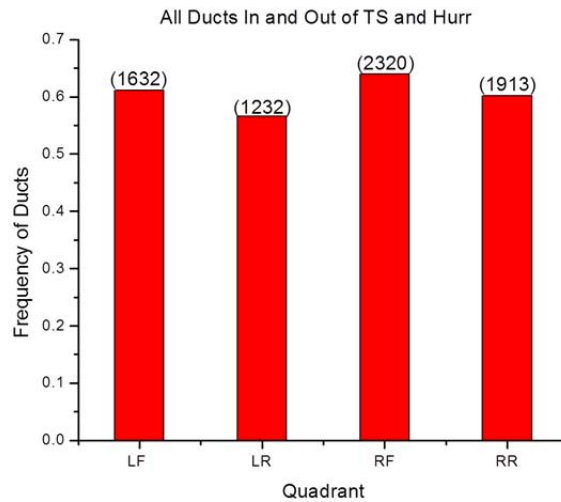


Figure 15. Total frequency of ducting in and out of both tropical storms and hurricanes by quadrant. The number above each column is the total soundings with ducts observed.

1. Ducting Inside Hurricanes

The following five figures in this section describe the ducting statistics for ducting inside hurricanes, which is the category with the most data (4511 profiles) from this dataset. The data is analyzed for both quadrant and type of duct to fully describe quadrant and type of duct for frequency, duct strength and duct height. Figure 16 displays the same frequency of ducting by quadrant. Comparing this result with Figure 15 using data from all quadrants, we cannot identify any difference with significance.

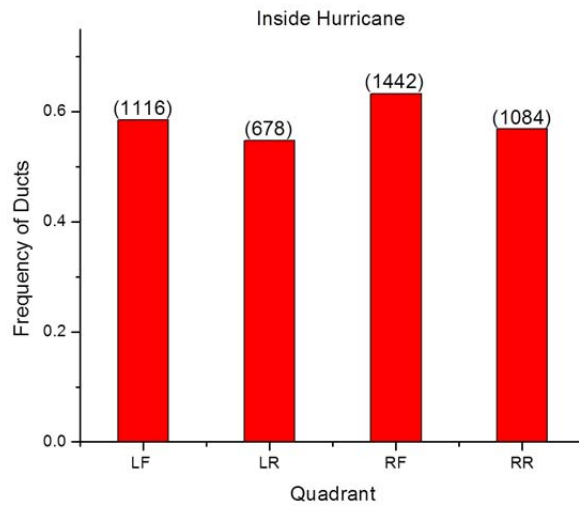


Figure 16. Total frequency of ducting inside hurricanes by quadrant.

Figure 17 shows the total frequency of ducting by quadrant and with duct type. Again, the frequency variation with quadrant is very similar to that shown in Figure 15. We do not identify any quadrant preference from insider hurricane, either.

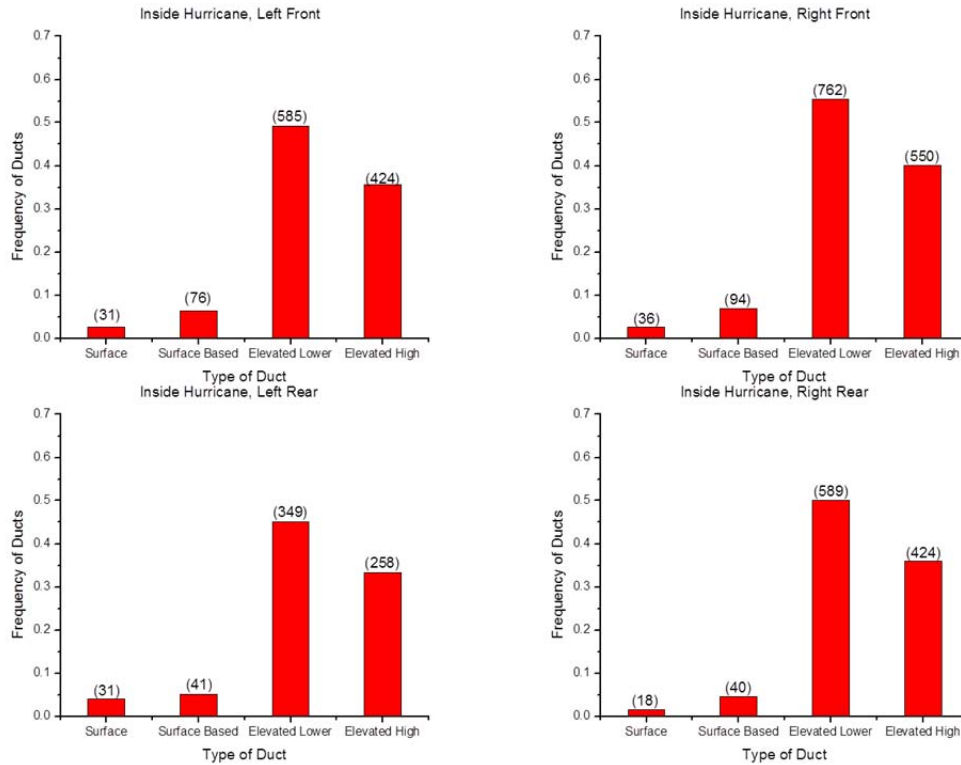


Figure 17. Total frequency of ducting inside hurricanes for each type of duct by quadrant.

Figure 18 displays the mean duct heights of the inside hurricane ducts. There is no preference statistically to any side or quadrant of a hurricane to show a significant change in the height of the duct for each duct type. The lack of preference for the side of hurricanes is consistent with results earlier in this thesis. Figure 19 below is a histogram of the results inside the hurricane for the elevated lower duct type; it shows that the duct height has a mode of around 600 meters. This distribution is apparently right skewed with some rather high ducts in all quadrants. Similar distribution is seen in Figure 20 for the elevated high ducts. The distribution has a long tail to the right in all four quadrants, showing the very high ducts of up to 6000 meters found in some soundings. The ducts of this height are only found inside the hurricane and are attributed to the highly convective structure inside a hurricane.

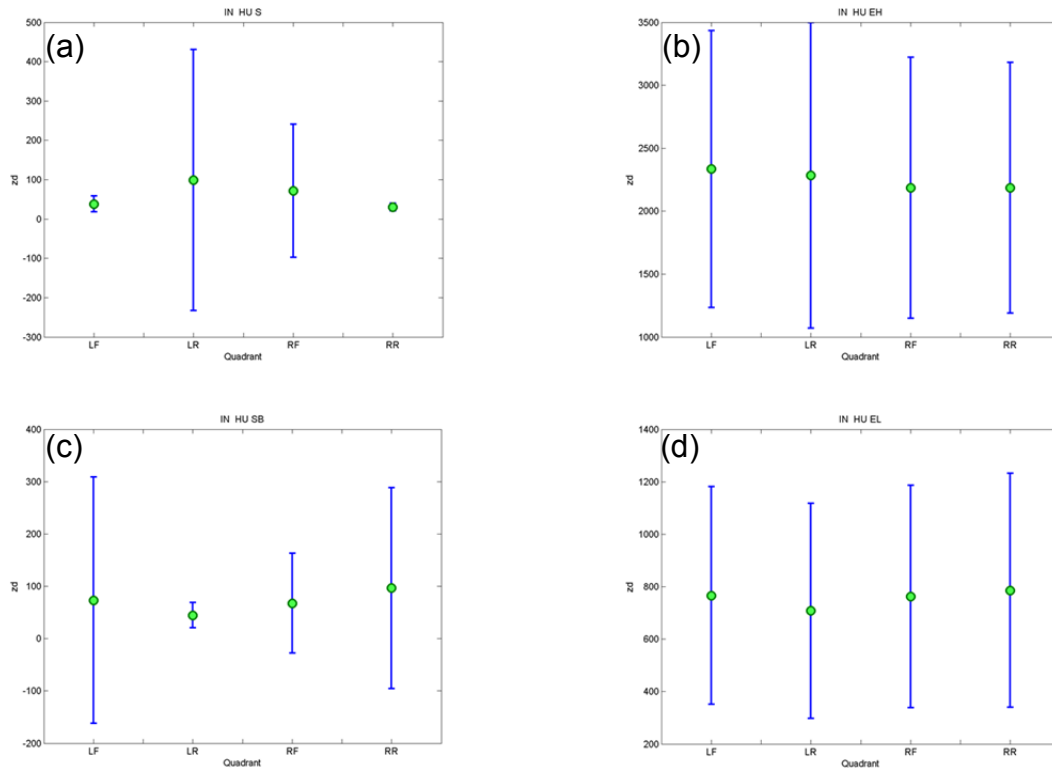


Figure 18. Mean duct height and standard distribution for each type of duct inside of a hurricane by quadrant. (a) surface duct, (b) elevated high ducts, (c) surface-based duct and (d) elevated low ducts. Results in (a) are not statistically significant due to the low number of samples.

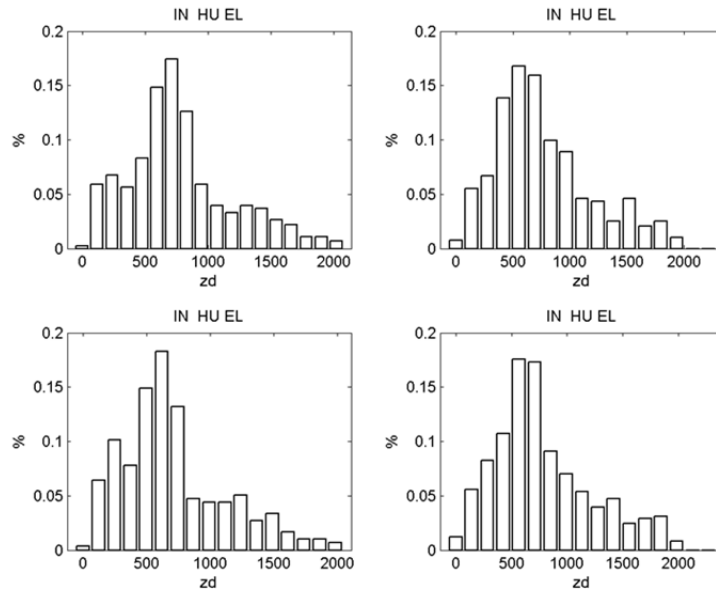


Figure 19. Histogram of the distribution of duct height in the elevated low ducts (EL) inside hurricanes by quadrant. The four graphs represent the corresponding quadrants of the storm: left front (LF), left rear (LR), right front (RF), and right rear (RR).

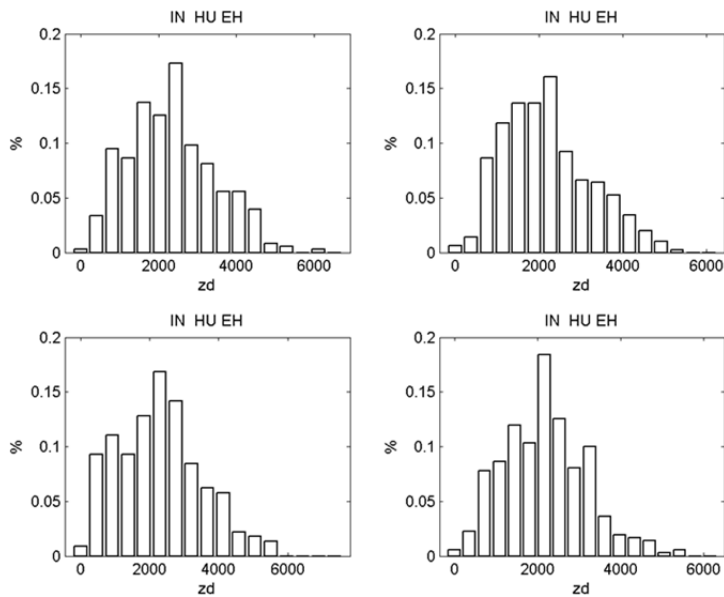


Figure 20. Same as in Figure 19, except for the elevated lower (EH) ducts inside hurricanes by quadrant.

The duct strength (dM) depicted in Figure 21 below is nearly equal among all types of ducting and quadrants. The mean value of approximately 5 M-units was nearly uniform across the quadrants and types for the well-mixed and highly convective structure inside the hurricane.

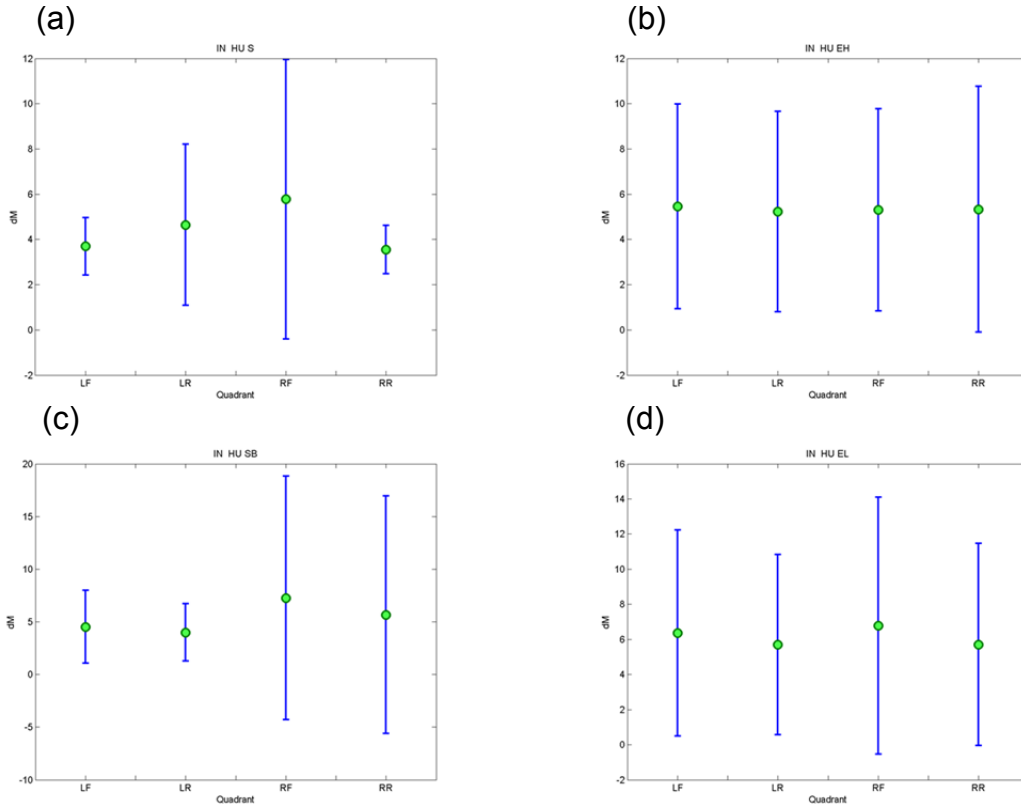


Figure 21. Same as in Figure 18, except duct strength (dM). Again, data from surface duct (a) should not be analyzed due to the small amount of data sample.

2. Outside Hurricane

The number of dropsondes outside the hurricane, a total of 3515, is the second largest group of the four storm-relevant categories. The previous thought was that the most conducive area for ducting to occur would be in the outer regions of the hurricane. The premise was the outer areas of the hurricane will be most affected by dry air entering the system as well as the outer areas being subject to dry air entrainment from land mass and upper latitudes. The overall

frequency (Figure 22 and 23), duct height (Figure 24) and duct strength (Figure 27) observed did not vary statistically compared to the inside hurricane dataset. For the Figures 22 through Figure 27 the analysis and values were consistent with the previous section from ducts inside hurricanes.

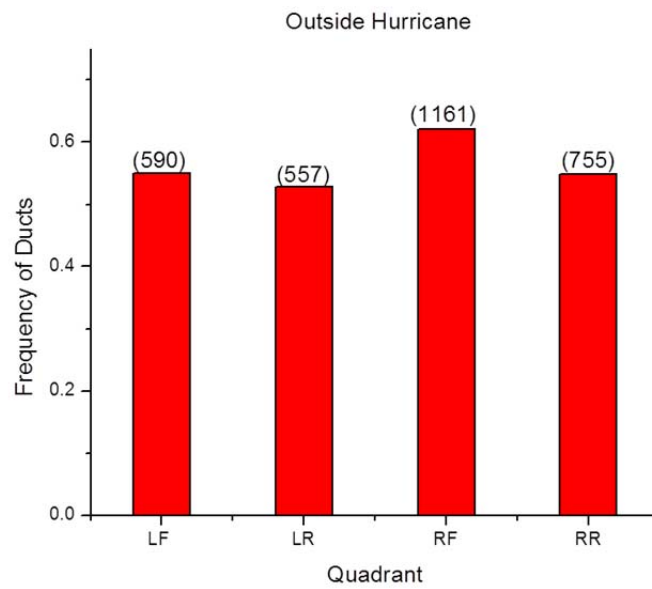


Figure 22. Same as Figure 16 except for ducts outside hurricanes.

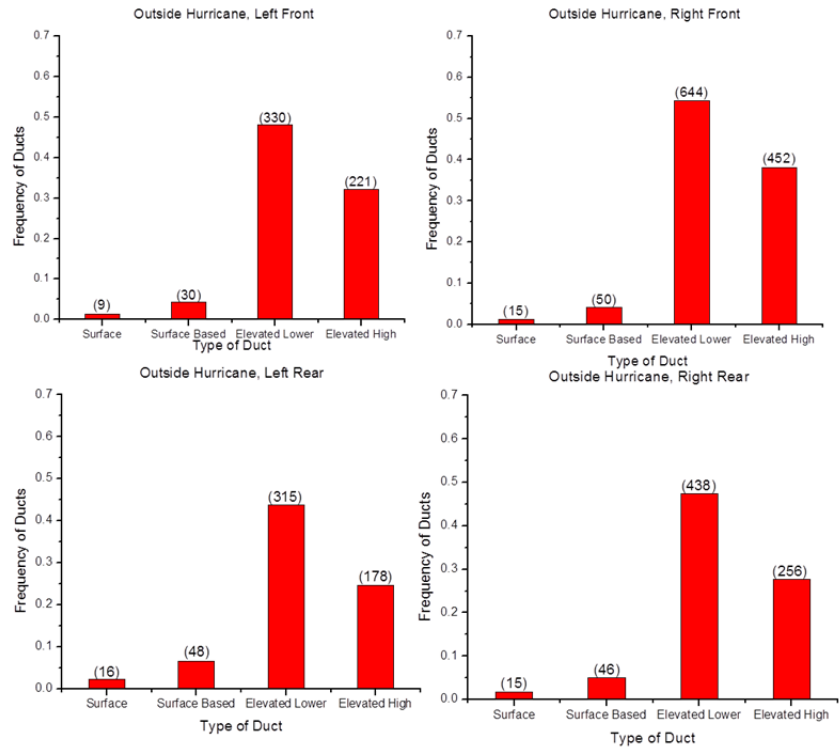


Figure 23. Same as Figure 17 except for ducts outside of hurricanes.

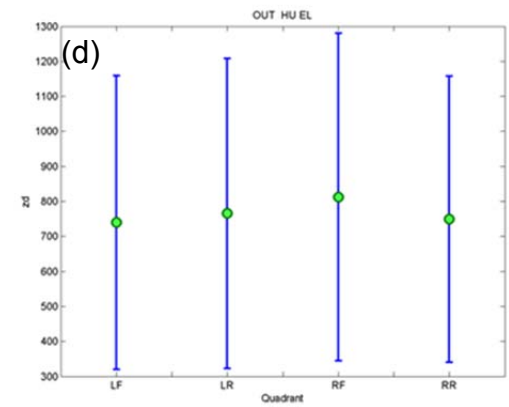
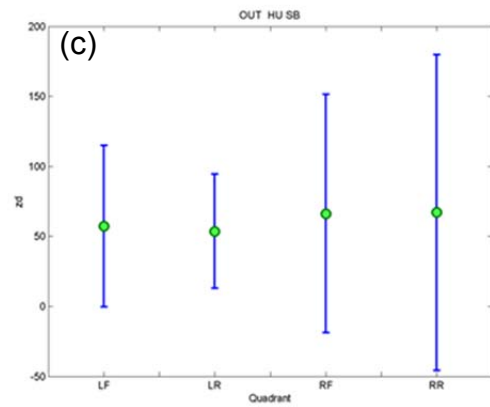
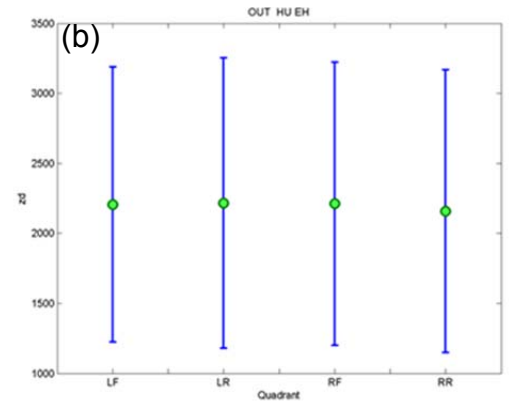
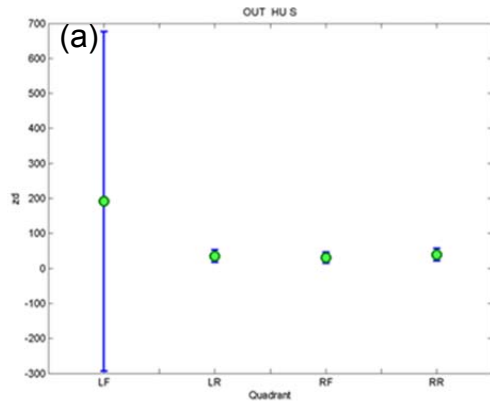


Figure 24. Figure Same as Figure 18 except for ducts outside of hurricanes.

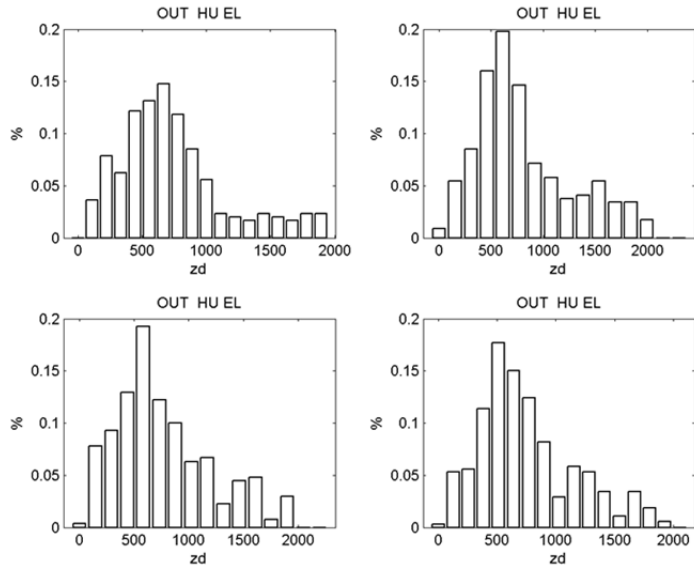


Figure 25. Same as Figure 19 except for ducts outside of hurricanes.

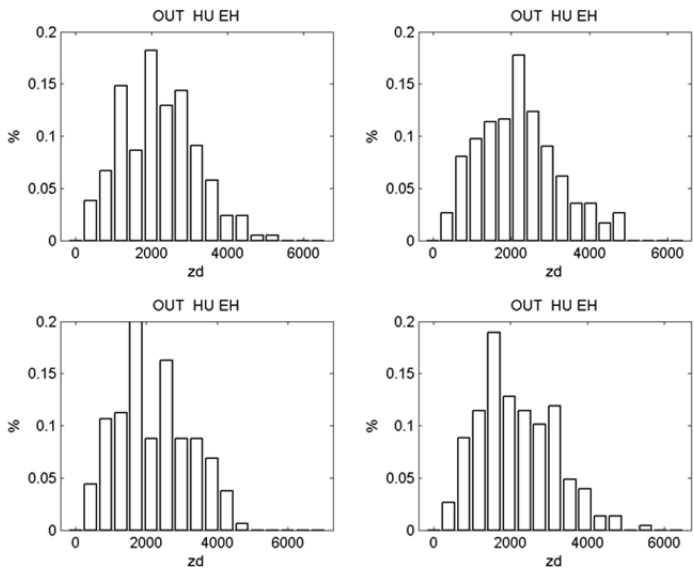


Figure 26. Same as Figure 20 except for ducts outside of hurricanes.

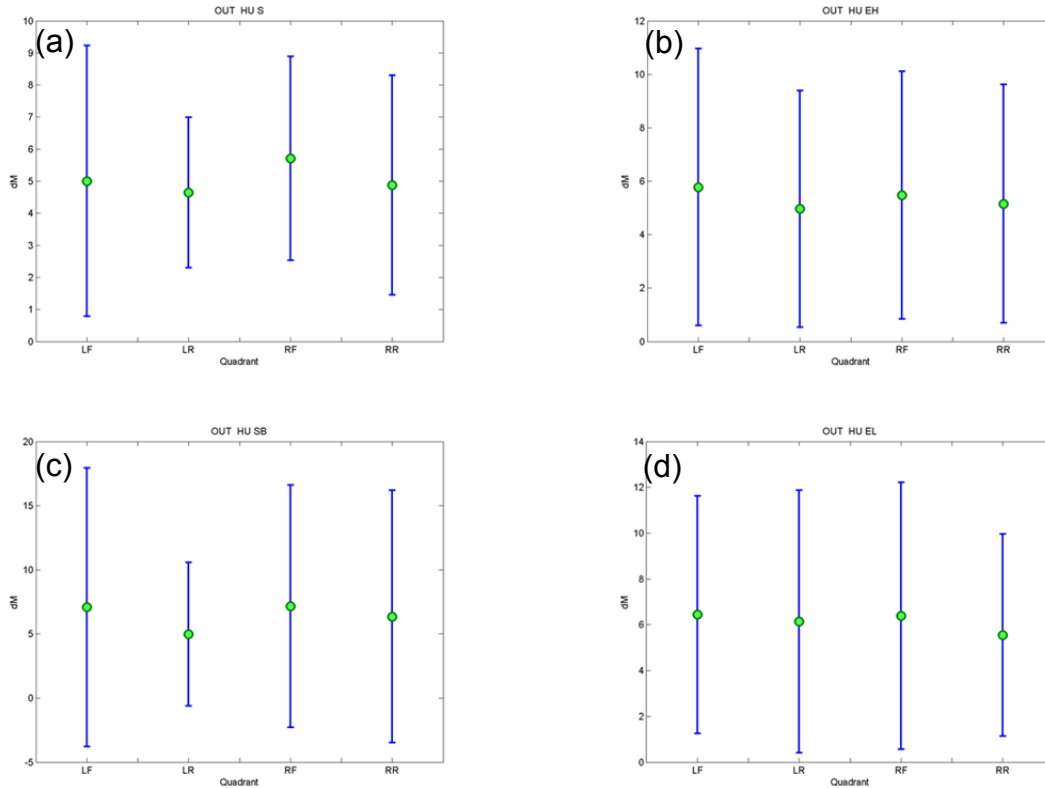


Figure 27. Same as Figure 21 except for ducts outside of hurricanes.

3. Inside Tropical Storm

The number of dropsondes inside the tropical storm, a total of 1962, is the third in total soundings of the four types in this section. The inside of the tropical storm was expected to behave similarly to the inside of a hurricane. The overall frequency, duct strength and duct height did not vary statistically compared to the other categories. The consistency of frequency (Figures 28 and 29) of ducting and the values of duct height (Figure 30) and duct strength (Figure 33) show nearly identical ducting conditions in tropical storms and in hurricane environments. Hurricanes and tropical storms both have strong convection that promote vertical mixing, resulting in similarities seem in this set of results (Figures 28–33) compared to Figures 16–21. The histogram (Figure 32) of the heights of ducting for the elevated high did show some skewing to the right for higher ducts but was not as severe as the hurricane data set.

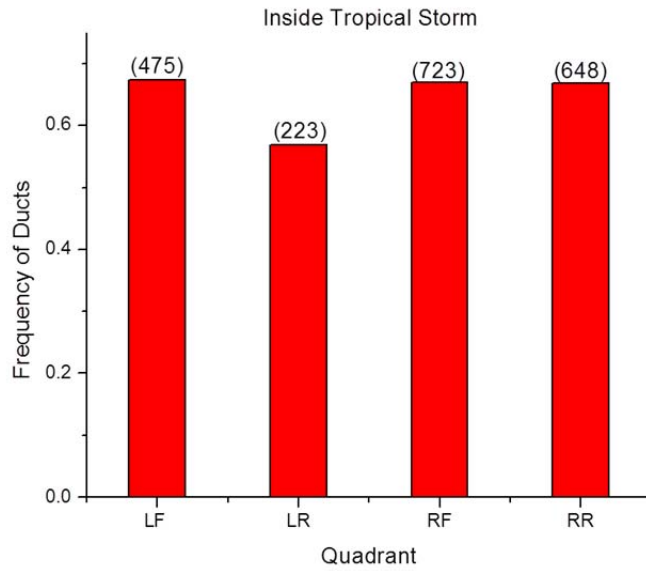


Figure 28. Total frequency of ducting inside tropical storms by quadrant.

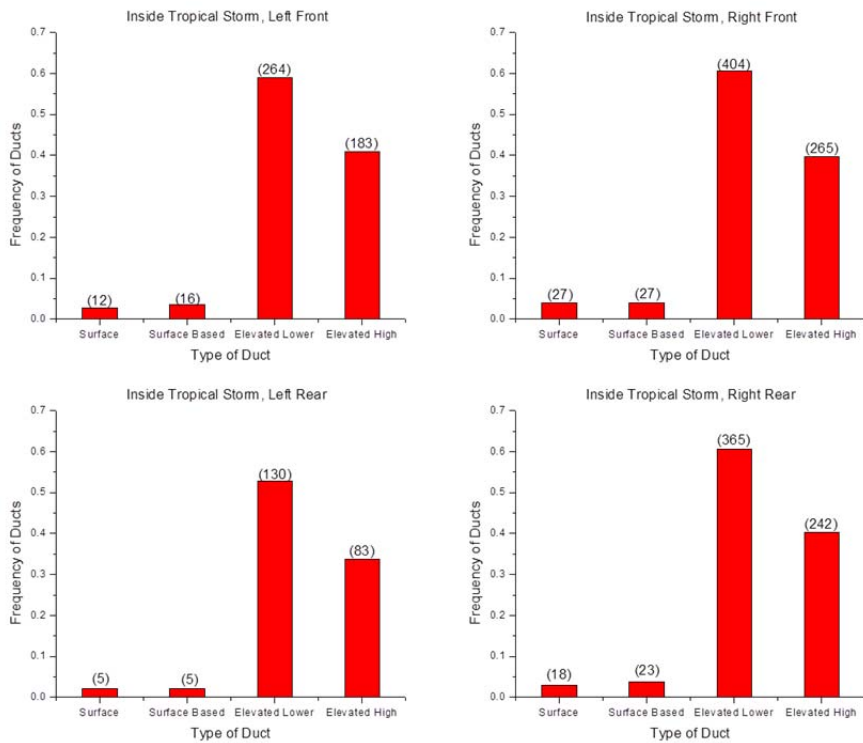


Figure 29. Total frequency of ducting inside tropical storms for each type of duct by quadrant.

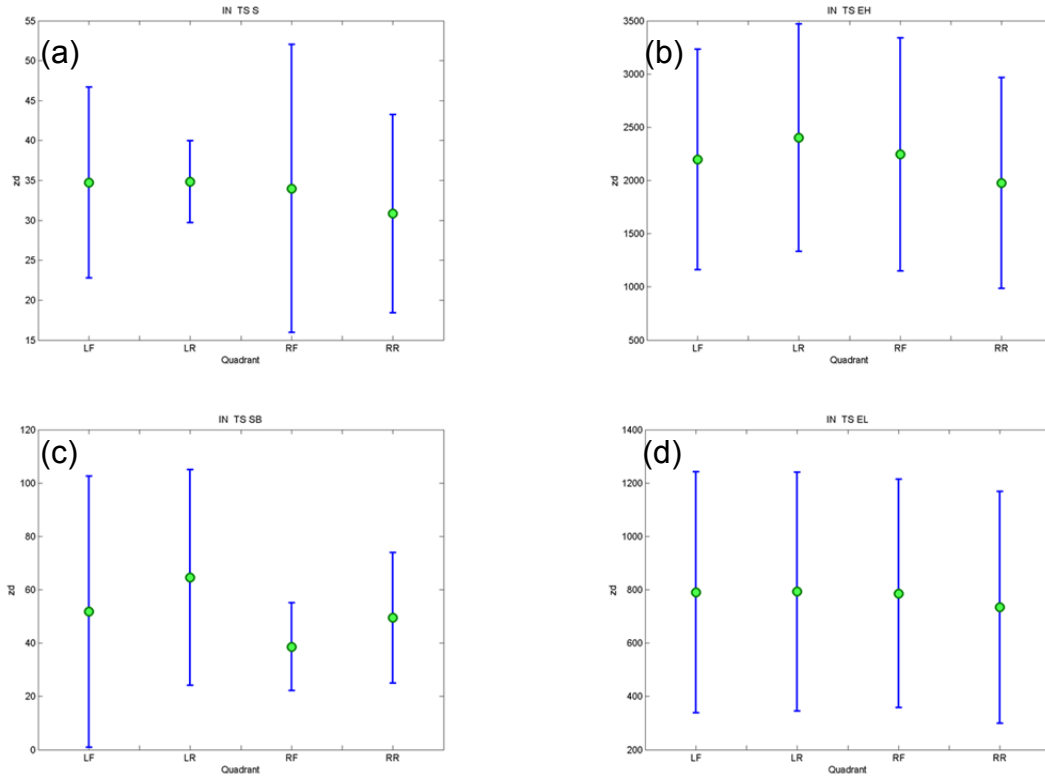


Figure 30. Mean duct height and standard distribution for each type of duct inside of a tropical storm by quadrant. (a) surface duct, (b) elevated high ducts, (c) surface-based duct and (d) elevated low ducts. Results in (a) and (b) are not statistically significant due to the low number of samples.

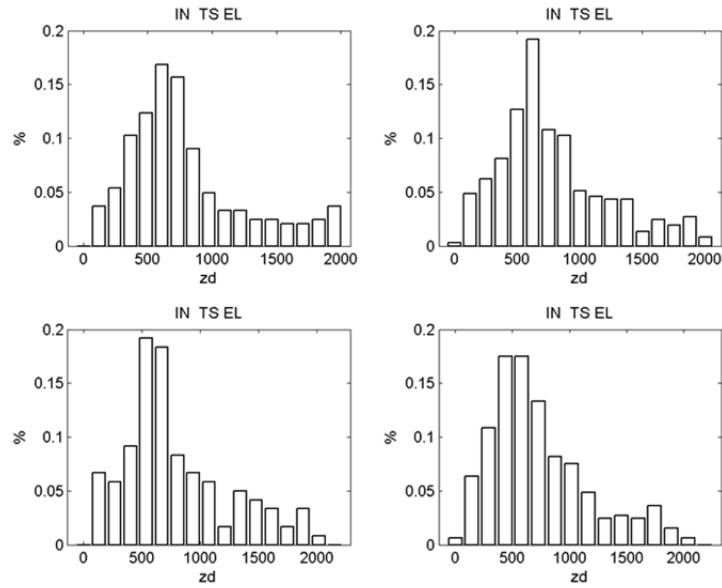


Figure 31. Histogram of the distribution of duct height in the elevated low (EL) ducts inside tropical storms by quadrant. The four graphs represent the corresponding quadrants of the storm: left front (LF), left rear (LR), right front (RF), and right rear (RR).

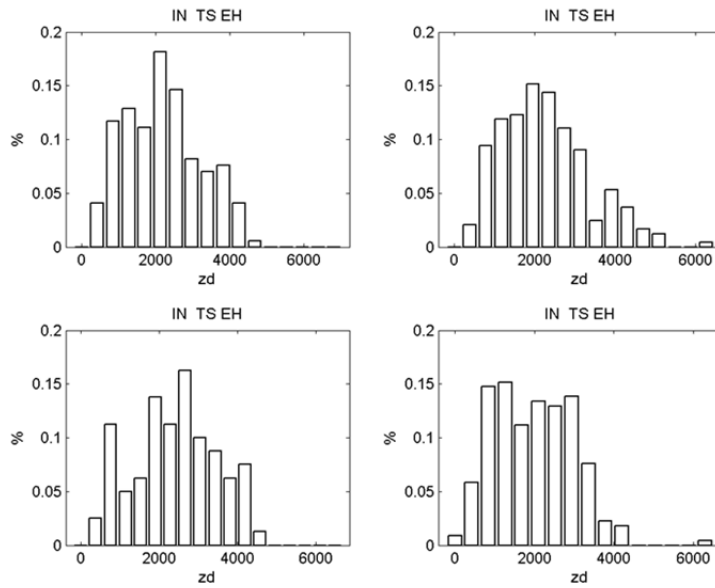


Figure 32. Histogram of the distribution of duct height in the elevated high (EH) ducts inside tropical storms by quadrant. The four graphs represent the corresponding quadrants of the storm: left front (LF), left rear (LR), right front (RF), and right rear (RR).

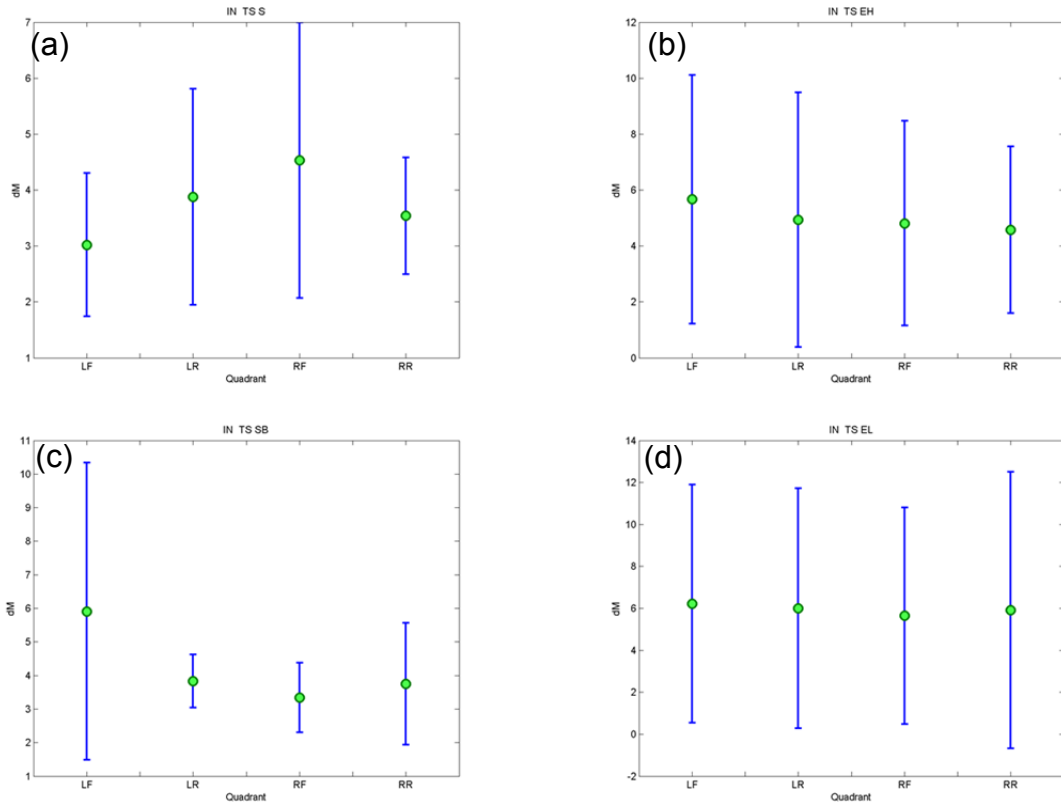


Figure 33. Mean duct height and standard distribution for each type of duct inside of a tropical storm by quadrant. (a) surface duct, (b) elevated high ducts, (c) surface-based duct and (d) elevated low ducts. Results in (a) and (b) are not statistically significant due to the low number of samples.

4. Outside Tropical Storm

The number of dropsondes outside the tropical storm, a total of 1666, is the fourth in total soundings of the four types in this section. Outside of a tropical storm there was expected to be a change in the frequency of ducting similar to the area outside of the hurricane discussed earlier. The interaction of tropical storms with midlatitude air masses should increase dry air interaction inside the region, but a significant increase in ducting was not observed. This was the only location where the frequency of the left side of the storm had a higher frequency of ducting. However, the difference in occurring frequency was less than 5%. Giving the relatively low number of samples in this subset of data, this should not

be considered a major finding until we obtain more data samples. The right rear of the outside tropical storm shows higher frequency of ducting which is consistent with wraparound dry air entrainment, which occurs when a tropical storm moves into mid-latitudes. There is also a right front higher frequency of elevated high ducting, which is attributed to the interactions in higher latitudes. The elevated lower and elevated high ducts display slightly greater duct strength of 6. The change is not significant and can be attributed to the greater radius of the dropsondes in the dataset and the locations further from a much warm-core like the hurricane.

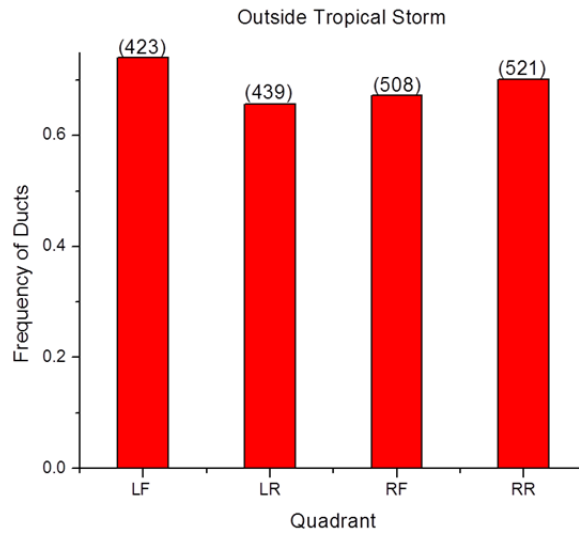


Figure 34. Same as Figure 28 except for ducts outside of tropical storms.

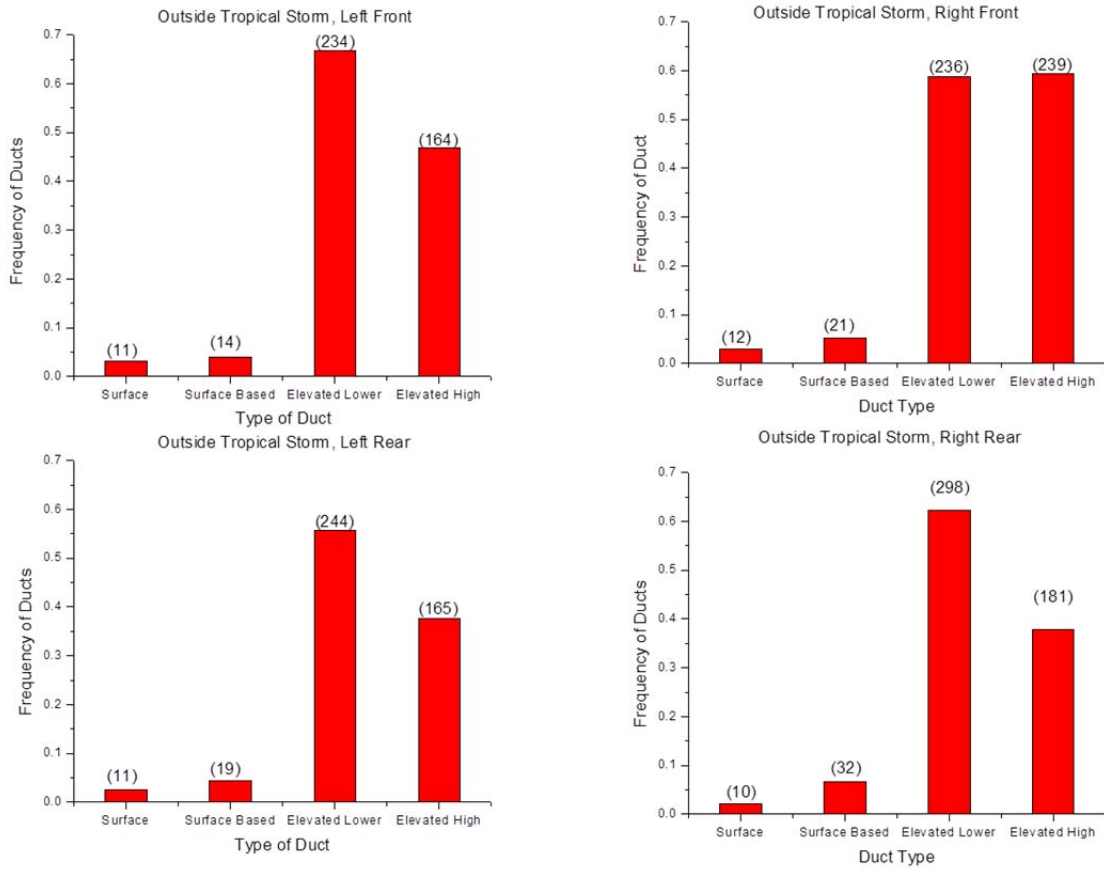


Figure 35. Same as Figure 29 except for ducts outside of tropical storms.

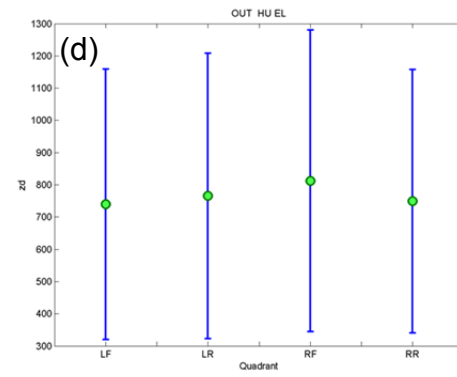
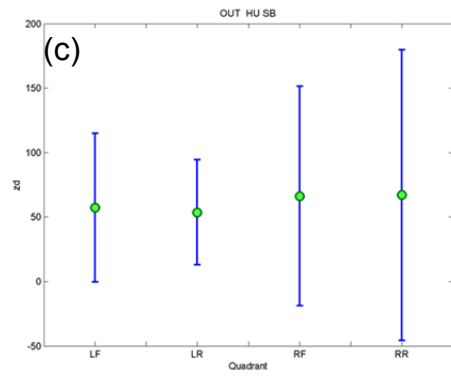
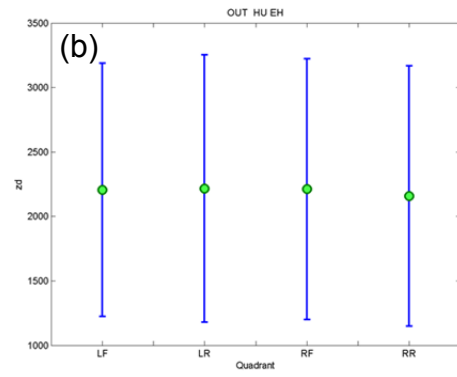
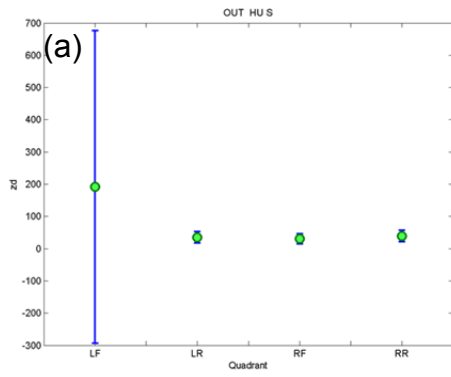


Figure 36. Same as Figure 30 except for ducts outside of tropical storms.

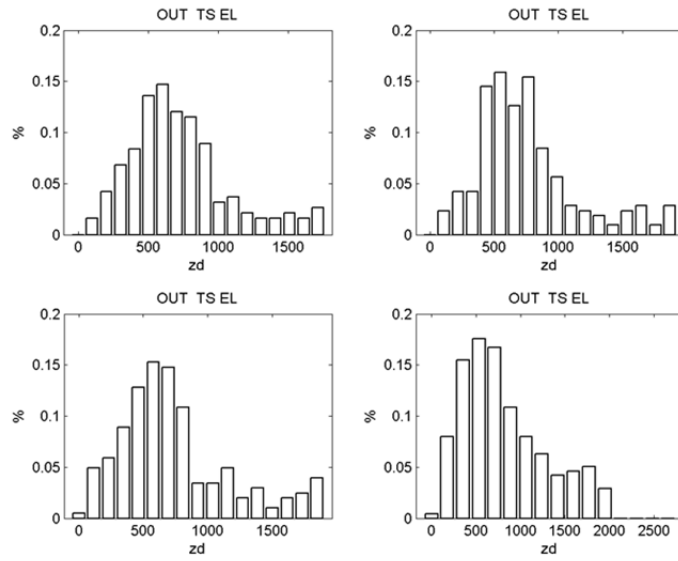


Figure 37. Same as Figure 31 except for ducts outside of tropical storms.

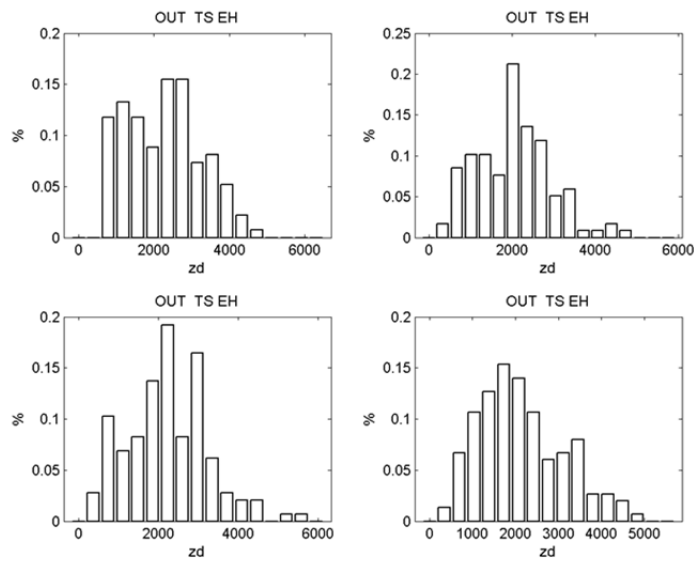


Figure 38. Same as Figure 32 except for ducts outside of tropical storms.

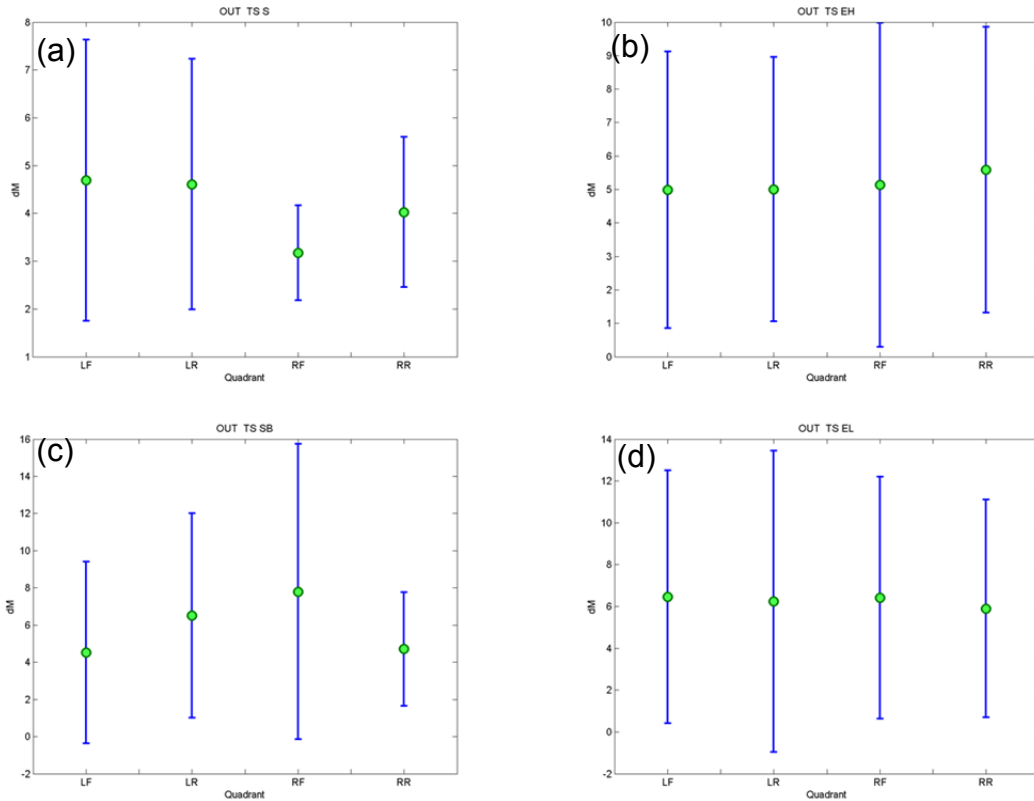


Figure 39. Same as Figure 33 except for ducts outside of tropical storms.

D. DUCTING CONDITIONS IN DIFFERENT GEOGRAPHIC REGIONS

This section investigates the possibility of different ducting characteristics in different geographic regions. The objective is to analyze the ducting attributes in geographic regions set forth by Neese (2010). The reasoning was that synoptic effects in each region (Figure 40) might cause changes to the number of ducts. The overall data set was used for this section to identify the change in ducting attributes varies in different geographic regions. For example the East Coast Dry is a region where most storms have recurved, and are being influenced by dry air from the North American continent, and mid-latitude upper air interactions. The interactions would likely cause dry air entrainment and cause elevated ducting to occur. The Deep Tropics and the Main Development

Region were expected to be nearly uniform, moist and warm, which would inhibit ducting in the region.

Eighty-four percent of the droponde dataset (Table 4) was deployed in the geographic regions defined below. The geographic regions were then investigated for the frequency of ducting by region (Figure 41).

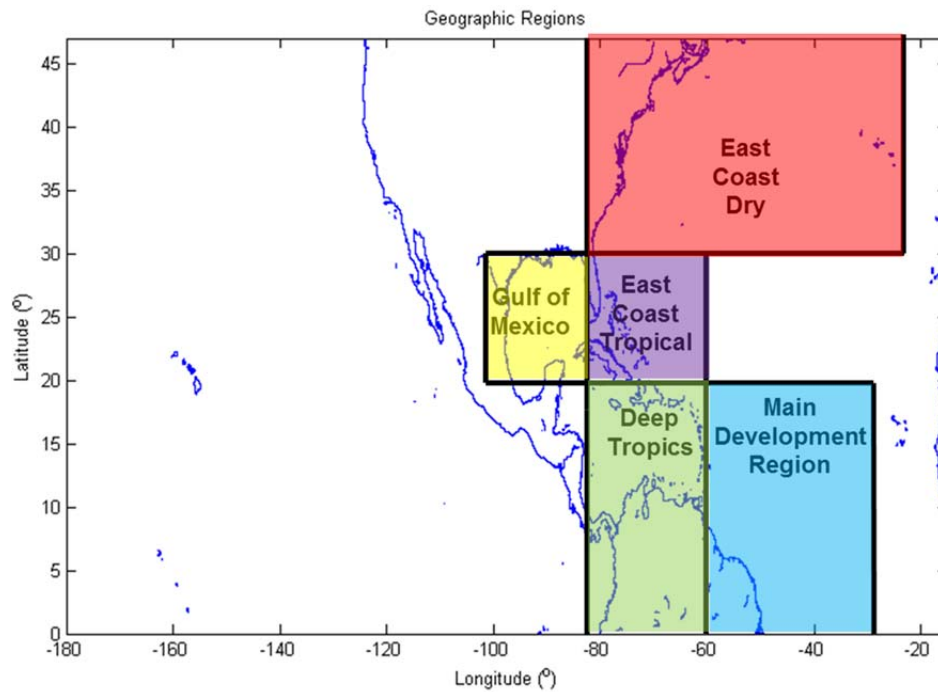


Figure 40. Geographic regions of tropical disturbances as described by Neese (2010). The regions are separated by areas, which are geographically significant to the tropical storm and hurricane. Each region is dynamically different with areas, which are much less impacted by interaction with the continent and others, which are more.

Geographic Region	Profiles	Ducts
Gulf of Mexico	4291	4164
East Coast Dry	1630	1488
East Coast Tropical	3695	3716
Deep Tropics	1151	1121
Main Development Region	712	799
Total	11479	11288

Table 4. Total profiles and ducts by geographic regions.

Using the entire data set and separating by region, we have found negligible differences in ducting (Figure 41). The frequency of surface and surface-based ducts was 2% and 4% for each region. The frequency of elevated lower ducts was between 52% and 61% in all but one region. The only region where ducting was slightly above 60% was in the Main Development Region. This is statistically not significant as the Main Development Region has the lowest number of data points and is only slightly above the mean of all ducting of elevated ducts. All regions are nearly equal to the overall mean frequency of each duct type.

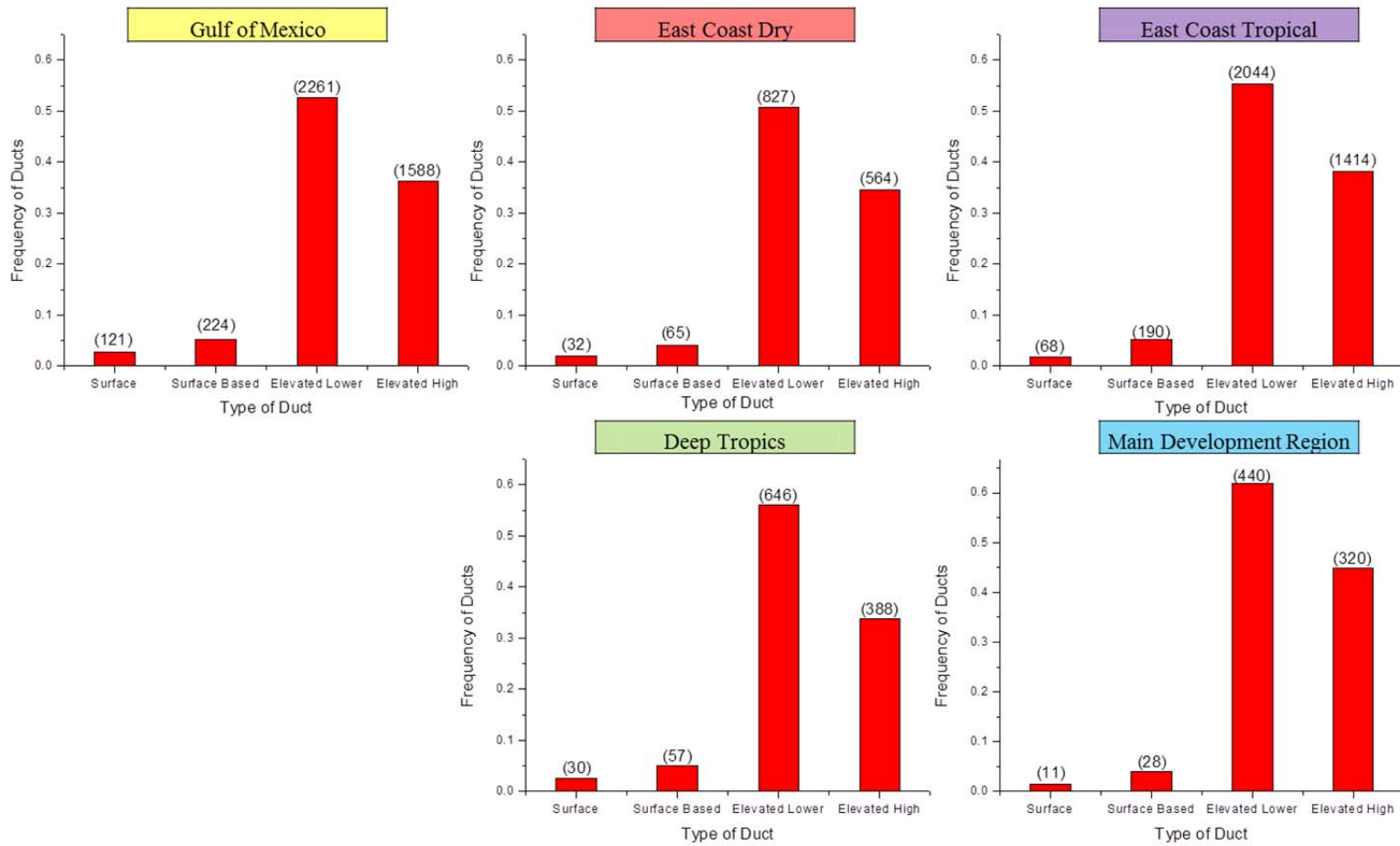


Figure 41. Frequency of ducting by type of duct in various geographic regions.

E. DISCUSSIONS

In this section, the NCAR GPS Dropsonde Dataset findings were compared to past climatology by Engeln and Teixeira (2004), which produced a ducting climatology using 5 years of global analysis data. For the months of June through November, which is the hurricane season, the occurrence of ducting over the majority of the Atlantic Ocean was found to be approximately 20% in the main region where ducting was analyzed in this study (outlined in the red box in Figure 42 below). The observed occurrence in the NCAR GPS Dropsonde Dataset was around 60%. The significant difference between the observed ducting and climatology can be attributed to the very low occurrence of a hurricane or tropical storm in the region at any given time as well as little study into the ducting of tropical storms and hurricanes.

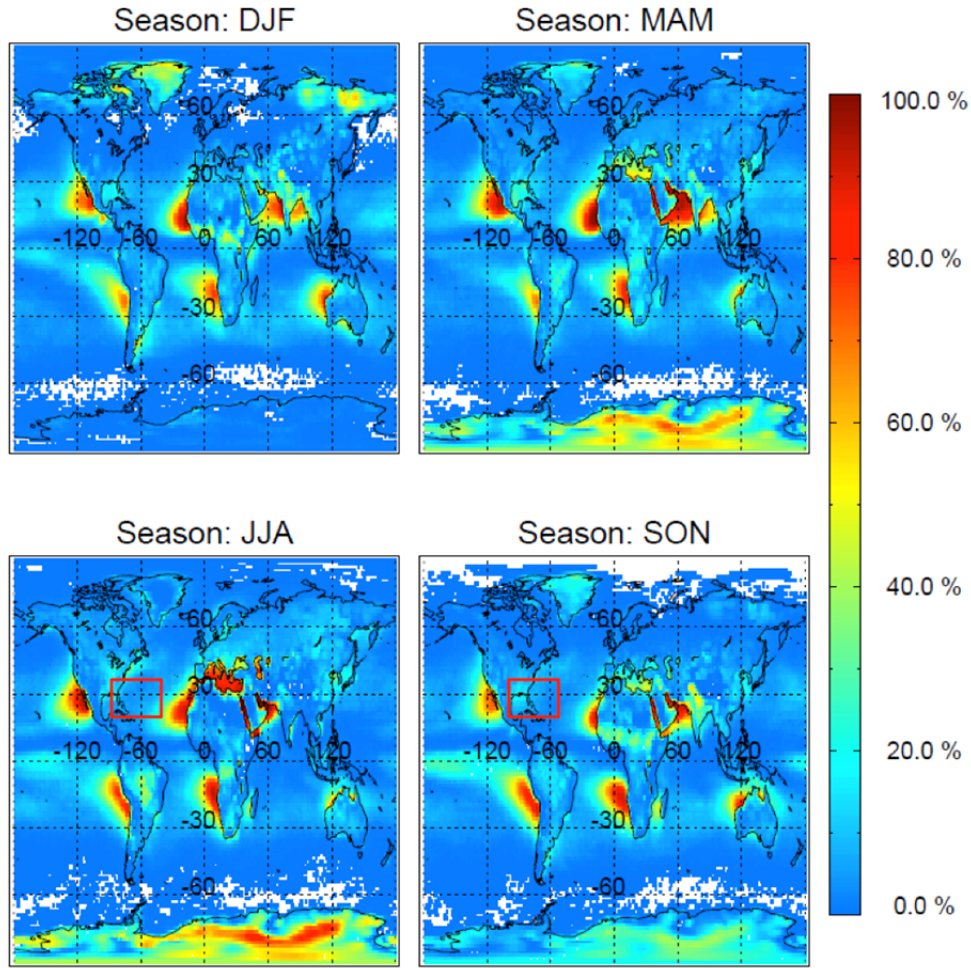


Figure 42. A Depiction of Ducting Climatology derived from 5 years of ECMWF Global Analysis (Engeln and Teixeira, 2004). The red box above outlines the main area of dropsondes in this study.

THIS PAGE INTENTIONALLY LEFT BLANK

V. SUMMARY, CONCLUSIONS AND RECOMMENDATIONS

A. SUMMARY AND CONCLUSIONS

The goal of the study was to describe ducting in strong convective storms over the Atlantic Ocean and research on whether the hurricane environment is conducive for ducting. This study utilized the NCAR QC'd GPS Dropsonde Dataset of 13664 vertical profiles from 1996 through 2012. This study determined 60.7% of dropsonde profiles contained at least one duct. There were a total of 16834 observed ducts, which includes multiple ducts in a profile. The analysis included the separation of ducting into type of duct and found that each had the following frequency: surface ducts (300) 2%, surface-based ducts around (668) 5%, elevated ducts (7866) 58%. The dataset was separated and investigated for inside and outside of tropical storms and hurricanes, as well as by quadrant with respect to the storm movement. The final investigation involved the geographic region of the individual dropsonde. For all the different areas, location, type of duct and regions the overall statistical occurrence of ducting did not change significantly.

This study concurs with Ding et al. (2013) that ducting in the tropical storm and hurricane affected areas occurs frequently and is an area conducive for duct formation. This study showed that ducting occurs about 60% of all the profiles, similar to the 57% rate in Ding et al. (2013). The comparison of this study's findings to the climatology in the previous chapter also displays that the finding of 60% frequency of ducting is multiple times greater than in climatology and tropical storm and hurricanes are therefore more conducive to ducting than previously thought. Results from both this and the Ding et al. (2013) paper displayed very low occurrence of surface ducting in the hurricane and tropical storm environment. The major difference between the findings from the data in this study and Ding et al. (2013) was the preference of ducting by quadrant of the storm for frequency and strength of ducting. This was not found in this study by evaluating the NCAR GPS Dropsonde dataset. The difference is likely due to the

size of the two datasets. This study used a much larger dataset (13664 compared to 357 sondes in the Ding et al. paper).

B. RECOMMENDATIONS

Further research using the NCAR GPS Dropsonde dataset is necessary for more EM/EO investigation. An additional separation of the profiles is by relative distances to the coast, which may reveal any differences in duct attributes. Other uses for this dataset are to study the hurricane boundary layers.

LIST OF REFERENCES

- Babin, S. M., 1996: Surface duct height distributions for Wallops Island, Virginia, 1995–1996. *J. Appl. Meteor.*, **35**, 86–93.
- Battan, L. J., 1959: *Radar Observation of the Atmosphere*. The University of Chicago Press, 324 pp.
- Brooks, I. M., A. K. Goroch, and D. P. Rogers, 1999: Observations of Strong Radar Ducts Over the Persian Gulf. *J. Appl. Meteor.*, **38**, 1293–1310.
- burk, s. d., and w. t. thompson, 1997: mesoscale modeling of summertime refractive conditions in the Southern California Bight. *J. Appl. Meteor.*, **36**, 22–31.
- Cook, J., 1991: A sensitivity study of weather data inaccuracies on evaporation duct height algorithms. *Radio Sci.*, **26**, 731–746.
- Ding, J., J. Fei, X. Huang, and X. Cheng, 2013, Observational occurrence of tropical cyclone ducts from GPS Dropsonde Data, *J. Appl. Meteor. Climatol.*, **52**, 1221–1236.
- Fairall, C. W., K. L. Davidson, G. E. Schacher, and T. M. Houlihan, 1978, Evaporation Duct Height Measurements in the Mid-Atlantic, Monterey, California. Naval Postgraduate School, <http://hdl.handle.net/10945/29858>
- Frederickson, P. A., J. T. Murphree, and K. L. Twigg, A. Barrios, 2008, A modern global evaporation duct climatology, *2008 Conference on Radar*
- Hock, T.F., and J.L. Franklin, 1999, The NCAR dropwindsonde, *Bull. Amer. Meteor. Soc.* Vol. **80**, No. 3, 407–420.
- Kepert, J.D., 2010 Slab and height resolving models of the tropical cyclone boundary layer. Part 1: Comparing the simulations. *Q. J. R. Meteorol. Soc.* **136**, 1686–1699.
- Laing, A., and J. Evans, 2011, Introduction to Tropical Meteorology. University Corporation for Atmospheric Research. http://www.meted.ucar.edu/tropical/textbook_2nd_edition/index.htm
- Newton, D. A., 2003: COAMPS modeled surface layer refractivity at the Roughness and Evaporation Duct Experiment 2001. M.S. dissertation, Dept. of Meteorology, Naval Postgraduate School
- Smith, R.K., and M.T. Montgomery, 2010, Hurricane boundary-layer theory. *Q. J. R. Meteorol. Soc.* **136**, 1665–1670.

Turton, J. D., and D. A. Bennets, and S. F. G. Farmer, 1988: An introduction to radio ducting. *Meteor. Mag.*, **117**, 245–254.

Zhang, J.A., R. F. Rogers, D. S. Nolan, and F. D. Marks, 2011: On the Chareacteristic Height Scales of the Hurricane Boundary Layer. *Bull. Amer. Meteor. Soc.* Vol. **139**, 2523–2534.

INITIAL DISTRIBUTION LIST

1. Defense Technical Information Center
Ft. Belvoir, Virginia
2. Dudley Knox Library
Naval Postgraduate School
Monterey, California